Global Monitoring and Forecasting of Biomass-Burning Smoke: Description of and Lessons From the Fire Locating and Modeling of Burning Emissions (FLAMBE) Program

Jeffrey S. Reid, Edward J. Hyer, Elaine M. Prins, Douglas L. Westphal, Jianglong Zhang, Jun Wang, Sundar A. Christopher, Cynthia A. Curtis, Christopher C. Schmidt, Daniel P. Eleuterio, Kim A. Richardson, and Jay P. Hoffman

***Abstract*—Recently, global biomass-burning research has grown from what was primarily a climate field to include a vibrant air quality observation and forecasting community. While new fire monitoring systems are based on fundamental Earth Systems Science (ESS) research, adaptation to the forecasting problem requires special procedures and simplifications. In a reciprocal manner, results from the air quality research community have contributed scientifically to basic ESS. To help exploit research and data products in climate, ESS, meteorology and air quality biomass burning communities, the joint Navy, NASA, NOAA, and University Fire Locating and Modeling of Burning Emissions (FLAMBE) program was formed in 1999. Based upon the operational NOAA/NESDIS Wild-Fire Automated Biomass Burning Algorithm (WF_ABBA) and the near real time University of Maryland/NASA MODIS fire products coupled to the operational Navy Aerosol Analysis and Prediction System (NAAPS) transport model, FLAMBE is a combined ESS and operational system to study the nature of smoke particle emissions and transport at the synoptic to continental scales. In this paper, we give an overview of the FLAMBE system and present fundamental metrics on emission and transport patterns of smoke. We also provide examples on regional smoke transport mechanisms and demonstrate that MODIS optical depth data assimilation provides significant variance reduction against observations. Using FLAMBE as a context, throughout the paper we discuss observability issues surrounding the biomass burning system and the subsequent propagation of error. Current indications are that regional particle emissions estimates still have integer factors of uncertainty.**

Manuscript received March 18, 2009; revised June 12, 2009. First published August 18, 2009; current version published October 28, 2009. This work was supported by the National Aeronautics and Space Administration Interdisciplinary Science Program and the Office of Naval Research Codes 32 and 35. The FLAMBE program is funded by the NASA Interdisciplinary Science Program and the Office of Naval Research Code 322. J. Wang's participation in this paper was supported by the NASA New Investigator Program and Radiation Science Program.

J. S. Reid, D. L. Westphal, C. A. Curtis, and K. A. Richardson are with the Naval Research Laboratory, Monterey, CA 93943 USA (e-mail: jeffrey.reid@nrlmry.navy.mil; douglas.westphal@nrlmry.navy.mil; curtis@nrlmry.navy.mil; kim.richardson@nrlmry.navy.mil).

E. J. Hyer is with the University Corporation for Atmospheric Research Visiting Scientist Programs, Naval Research Laboratory, Monterey, CA 93943 USA (e-mail: ehyer@ucar.edu).

E. M. Prins, C. C. Schmidt, and J. P. Hoffman are with the Cooperative Institute for Meteorological Satellite Studies, University of Wisconsin, Madison, WI 53706 USA (e-mail: elaine.prins@ssec.wisc.edu; chris.schmidt@ssec.wisc.edu; jhoffman1@wisc.edu).

J. Zhang is with the Department of Atmospheric Sciences, University of North Dakota, Grand Forks, ND 58201 USA (e-mail: jzhang@aero.und.edu).

J. Wang is with the Department of Geosciences, University of Nebraska, Lincoln, NE 68508 USA (e-mail: jwang7@unlnotes.unl.edu).

S. A. Christopher is with the Department of Atmospheric Sciences, University of Alabama, Huntsville, AL 35806 USA (e-mail: sundar@nsstc.uah.edu).

D. Eleuterio is with the Office of Naval Research, Arlington, VA 22203 USA.

Color versions of one or more of the figures in this paper are available online at http://ieeexplore.ieee.org.

Digital Object Identifier 10.1109/JSTARS.2009.2027443

***Index Terms*—Aerosol forecasting, biomass burning, modeling, satellite applications.**

I. Introduction

BIOMASS burning has an important history in global climate and Earth Systems Science (ESS) studies with thousands of manuscripts on the topic. Synoptic scale biomass burning plumes are also gaining recognition for their importance to air quality and weather. With strengthening air quality regulations, intercontinental transport issues once considered secondary have become more significant. Ozone from Siberian forest fires can impact air quality in the Pacific Northwest United States [1]; smoke from Central America and the Yucatan Peninsula impacts air quality from Texas to Georgia [2], [3]; some North American and Siberian plumes have even been shown to impact the eastern Atlantic and Europe from the surface through the lower stratosphere [4]–[7].

In addition to air quality, the impact of aerosol particles on Numerical Weather Prediction (NWP) is coming into focus. This can be either directly through perturbations to heat budgets in the atmospheric column, or indirectly through microphysical processes affecting cloud processes. For example, large forest fires within North America can generate plumes so massive they cover much of the United States and perturb continental scale surface temperatures and boundary layer dynamics [8]. Regions of prevalent smoke, such as the Amazon, may exhibit boundary layer cloud impacts [9], [10]. It has been hypothesized with limited data that smoke may intensify severe thunderstorms [11], [12].

Improved characterization of major aerosol sources and transport is necessary to meet operational requirements for air quality and meteorological forecasting at the U.S. Navy's Fleet Numerical Meteorological and Oceanographic Center (FNMOC). Advances in NWP requirements are resulting in collinear research interests with the climate and ESS communities. There are common fundamental needs on aerosol sources, transport mechanisms, evolution processes, scavenging mechanisms, and impacts. With the incorporation of nonoperational NASA MODIS and AIRS data into operational systems, and soon the National Polar-orbiting Operational Environmental Satellite System (NPOESS), the Group on Earth Observations (GEO), and the Global Earth Observation System of Systems (GEOSS), remote sensing data sets are bridging these communities.

Despite similarities in the underlying science, applications have important differences in temporal and spatial scales. This has resulted in different methods and interpreted uncertainties. For example, the averaging or bulk parameterizations used in global transport/climate models can be justified by their respective scale (e.g., trends and projections). Uncertainties can be mitigated due to a process of compensating errors [13], [14]. ESS scientists alternatively can tolerate uncertainties so long as they use the best available information to understand fundamental processes. NWP needs an accurate estimation of constituent concentrations at individual points in time and space in a consistent and timely manner. This may result in simplified physics or incomplete data so long as the correct forecast is generated (i.e., the ends justify the means).

The effects of biomass burning span a broad range of spatial and temporal scales and the problem is underdetermined with regard to sources, chemistry and the range of transport scales. Regardless of application, biomass burning is extraordinarily complex to fully physically parameterize. The joint Navy, NASA, NOAA, and university Fire Locating and Modeling of Burning Emissions (FLAMBE) project was formed specifically in order to bridge the climate, ESS and NWP research communities. The original goal was to investigate a physically consistent system of emissions, transport, and radiative impacts that could jointly serve the climate, ESS and NWP communities at the synoptic scale. This has since grown to include other air quality and other ESS related topics such as cloud and precipitation impacts. Research is performed in a diverse interdisciplinary manner. Focus has always been on technology development and the fundamental observability of the relevant processes.

Despite FLAMBE's use in many papers, it has not been comprehensively described in any published paper. Further, we are preparing for a number of operational improvements. The goal of this paper is to give a report on the current state of the FLAMBE system and its utilized satellite data sets. This paper hence presents a baseline record from which future papers will document operational improvement. As part of this description we also use FLAMBE as a context to discuss the nature of the fundamental observability of the global system as it relates to the bridging of the NWP, climate and ESS communities. Metrics regarding fire prevalence, emissions and transport are given and used to elucidate some issues confronting the biomass burning community at the synoptic to continental scale. Philosophies are presented that were gained from FLAMBE's nearly 10 years of existence. We conclude with a discussion of the large uncertainties that still exist in emissions estimates as well as FLAMBE's future direction.

II. FLAMBE System Goals and Philosophy

The FLAMBE project was first initiated in late 1999. This effort was jointly developed from the beginning through a NASA Interdisciplinary Science (IDS) program grant to study the extent to which biomass burning smoke's radiative and visibility impacts can be observed, and through an Office of Naval Research grant to study if smoke characteristics could be forecast. From its inception, FLAMBE focused on the pragmatic combination of satellite and model products, with realistic uncertainties and propagation of error. Original philosophy centered on the following.

i) Targeted Variables: The primary variables of interest are related to smoke particle radiative effects such as aerosol optical depth, surface and top-of-atmosphere fluxes, and atmospheric heating rates. NASA has since funded the areas of intercontinental transport of particulate matter and similar air quality issues, semi-direct/indirect forcing and precipitation impacts.

ii) Spatial and Temporal Scale: FLAMBE focuses on synoptic scale emissions and transport such as is found in the tropics and boreal regions. The monitoring and forecasting of local events is not a FLAMBE priority. Although much of our research is relevant to this area, the system currently is not designed to model point sources.

iii) Research to Operations: Remote sensing and modeling methods developed must be dual use for research as well as for operational production and NWP. Input data sets need to have near real time sources (< 6 hr, preferably < 1 hr), and routines need to be run within current computational limits. Hence, source estimation methodologies tend toward semi-empirical approaches and away from data-intensive mechanistic models.

iv) Source Function: It is well known that system efficacy is strongly related to the underlying source function. However, terms that go into a source function such as fire location, burned area, fuel load, and thermal characteristics are highly underdetermined. Some degree of uncertainty must be acceptable in order to achieve the constraint of iii).

v) Meteorology and Model Representation: Uncertainty in the source function is convolved with errors in modeled meteorology. If the model places a trough in the wrong position, predicts winds that are incorrect, or overestimates/underestimates precipitation, then there will be a direct impact on smoke simulation. Similarly, transport intricacies at the meso and microscale will not be well represented in a coarser scale model. Ideally the meteorology must be kept consistent so that error and bias can be accounted for between the meteorology and aerosol models.

vi) Remote Sensing: While the community has reached a pinnacle in the number of aerosol related satellite sensors and products, uncertainties are still not well quantified. Further, error statistics that are available tend to be global or highly isolated in nature and are difficult to apply to specific circumstances, locations or events in an automated fashion. Systematic variations in observational uncertainty, coupled with other contextual biases, can complicate and obscure the true observability of the system.

vii) Validation: Given the complexity of the observing system, there is difficulty in validating smoke products. Smoke has strong temporal, horizontal, and vertical gradients. This complexity is difficult to capture fully with the scattered and incongruent patchwork of validation data sources over the globe. Hence, the system should be no more complex than can be reasonably validated.

viii) Consistency: The aerosol model components need to be consistent. Research products, while often generated quasi-operationally, often have continuous adjustments

to algorithms or parameters. The recognition that multiple users are involved, especially nonscientists, forces a conservative attitude toward the balance between model complexity, upgrades and product consistency. Upgrades are made when the improvement in data quality is sufficient to justify the transitional efforts.

III. Description of the Current Flambe System

The core FLAMBE system has remained relatively consistent in methodology during the project term with occasional incremental upgrades. In order to provide traceability throughout the components as well as to study the fundamental observability of the biomass burning system, algorithms have been kept relatively simple. Geostationary (GOES) and polar orbiting (MODIS) active fire hotspot and characterization data is passed to a simple emissions algorithm that scales from a 1 km land use database. The resulting product is then fed into the Navy Aerosol Analysis and Prediction System (NAAPS) for transport and removal. NAAPS output is then analyzed with other observed data to study the biomass burning system. Recently, a MODIS optical depth data assimilation step has been added. The version of the system described here is now operational at the US Navy's Fleet Numerical Meteorological and Oceanographic Center (FNMOC) in Monterey CA. The exception is the aerosol optical depth data assimilation portion, which is nearing operational implementation at the time of writing of this paper.

A. Active Fire Hotspot Detection

Fire detection and climatologies have taken the form of manual records (e.g., deforestation logs, fire statistics, etc.), satellite and aircraft mapped burn scars, inverse studies, or active thermal detection by satellites. In the case of smoke forecasting applications, fire databases need to be updated before every model run. Hence, assessments are needed every 12–24 h at a minimum, with observations every 30 min to 1 h most preferable. An Active Fire Hotspot Detection is those satellite data pixels that show some elevated thermal anomaly above the regional background with sufficient confidence to explain it as being due to active fires. Fire Products are the host of derived properties from that active fire hotspot such as confidence, temperature, power, size, emissions properties, or metadata.

Currently there are only two satellite products that can meet global operational model requirements: the operational NOAA/NESDIS and preoperational UW-Madison Cooperative Institute for Meteorological Satellite Studies (CIMSS) geostationary Wildfire Automated Biomass Burning Algorithm (WF_ABBA, [15]–[18]), and the NASA/University of Maryland College Park MODIS fire product from the Terra and Aqua platforms available at the NASA Goddard Near Real Time Processing Effort (NRTPE) server [19], [20]. Both utilize a fire's thermal signature in the 3.7-3.9 μm window [21].

The geostationary and polar orbiting observing systems are complementary. While geostationary full disk fire products can provide high temporal resolution (15 min to 3 h) and capture the full diurnal cycle of burning, they have reduced spatial resolution in the infrared (~ 4 km nadir), particularly at limb viewing situations (up to 8 km at 60° latitude). Polar orbiter data from MODIS (and soon VIIRS) has higher spatial resolution (1 km, to 5 km on the limb) but with twice a day coverage (4 times for both Terra and Aqua). In high latitudes the two satellite types balance as polar orbiter coverage increases temporally and sensitivity for geostationary decreases. For both, detection efficiency varies with scan geometry: for geostationary sensors, this determines the geographic coverage while for polar orbiters, this affects the detection efficiency of specific observations [22], [23].

In addition to active fire detection, these systems permit retrieval of some sub-pixel fire characterization information. The WF_ABBA is based on the method of Dozier [21], where using the 3.9 and 11 μm bands and an estimate of the background nonfire pixel temperature, two nonlinear equations are solved for two unknowns, yielding instantaneous estimates of subpixel fire size and fire temperature [15]. These can then be integrated to estimate fire burn size or emission. An alternative approach relies on estimating the rate of energy release from a subpixel fire (the fire radiative power, or FRP), which has been shown to be proportional to fuel combustion under consistent, controlled conditions [24], [25]. FRP and the Dozier method use similar data inputs, and, therefore, there is a great deal of co-linearity between their products. Both methods are sensitive to precise determination of the background temperature [26], and evaluation of how to incorporate this information into the FLAMBE source function is ongoing.

Table I presents a list of current and potential geostationary satellite sensors suitable for fire detection. There are a number of independent groups now generating fire products from geostationary satellite data, including: GOES-E/-W (UW-Madison CIMSS; NOAA/NESDIS; Colorado State University; INPE – Brazil; Kings College – London); MET-8/9 (Council for Scientific and Industrial Research (CSIR) – South Africa; LandSAF; EUMETSAT; Kings College – London; NOAA/NESDIS; UW-Madison CIMSS; Telespazio – Rome; University of Rome; University of Valladolid); MTSAT-1R (NOAA/NESDIS; UW-Madison CIMSS); and FY-2C/2D (Chinese Meteorological Agency) .

For FLAMBE, we currently utilize WF_ABBA version 6.5. Originally designed for the GOES series of imagers, WF_ABBA has been run quasi-operationally since 2000 on GOES-8, 9, 10, 11, and 12 (as well as GOES-13 when available) over the western hemisphere and is now run operationally at NOAA NESDIS. In addition, a project is also underway to reprocess the GOES archive back to 1995 with version 6.5 of the WF_ABBA. Preoperational data production is also underway for the European Meteosat 8–9 (Europe and Africa) and Japanese MTSAT-1R (E and SE Asia) at CIMSS and NOAA/NESDIS. Algorithms for the Indian INSAT-3D, Korean COMS and Japanese MTSAT-2 are in development at CIMSS in preparation for the future deployment of these instruments.

Because of the interest in consistency and transition to operations, the FLAMBE program thus far has relied on geostationary WF_ABBA products where available with additional gap filling by MODIS. At the writing of this paper, GOES is used in the western hemisphere and MODIS in all other locations. It is expected that by the end of this year, Meteosat-9 and MTSAT-1R will be included in the FLAMBE data stream.

For comparison, Fig. 1 presents global seasonal GOES and MODIS Aqua active fire hotspot density. Included are raw counts [Fig. 1(a)], and data are also presented as active fire hotspot detects per overpass [Fig. 1(b)] to correct for coverage and temporal sampling. When comparing GOES and MODIS

TABLE I
CURRENT AND FUTURE GEOSTATIONARY CONSTELLATION OF FIRE OBSERVING SENSORS

Sensor	Center Longitude	3.9 µm IGFOV (km)	SSR (km)	3.9 µm Saturation (K)	Full Disk Coverage
Previous					
GOES-8 (USA)	75 °W	4 km	2.3 x 4.0	≥ 335	3 hr@
GOES-9 (USA)	135 °W	4 km	2.3 x 4.0	≥ 324	3 hr@
GOES-10 (USA)	135 °W	4 km	2.3 x 4.0	≥ 321	3 hr@
NOAA Operational					
GOES-10 (USA)	135 °W	4 km	2.3 x 4.0	≥ 321	3 hr@
GOES-11 (USA)	135 °W	4 km	2.3 x 4.0	≥ 340	3 hr@
GOES-12 (USA)	75 °W	4 km	2.3 x 4.0	≥ 336	3 hr@
CIMSS WF_ABBA Pre-operational					
Meteosat-8 (EU)	0°	4.8 km^	3.0 x 3.0	335	15 min.
Meteosat-9 (EU)	0°	4.8 km^	3.0 x 3.0	335	15 min.
MTSAT-1R (Japan)	140 °E	2 km*		~320	1 hr
Capable					
FY-2C (China)	105 °E	5 km		~ 330	30 min.
FY-2D (China)	86.5 °E	5 km		~ 330	30 min.
GOES-13 (USA)#	105 °W	4 km	2.3 x 4.0	≥ 340	3 hr
MTSAT-2 (Japan)	145 °E	5 km		~320 (TBD)	1 hr
Future					
COMS (2009- Korea)	128 °E	4 km		TBD	30 min.
INSAT-3D (2009-India)	83 °E (TBD)	4 km		TBD	30 min.
Electro-L N1 (2009-Russia)	76 °E	4 km		TBD	30 min.
Electro-L N2 (2010-Russia)	14.5 °E	4 km		TBD	30 min.
GOES-R/ABI (2015-USA)	75 or 135°W	2 km		400	5 min.
MTG (2015-EU)	0°	2 km		400-450	10 min.

Data derived in part from the Report of the 36th Meeting of the Coordination Group for Meteorological Satellites, Maspalomas, Gran Canaria, Spain, Nov. 3-7, 2008. Edited by CGMS Secretariat, EUMETSAT, Darmstadt, Germany [84, 85,86]. IGFOV represents the instantaneous ground field of view, value given is for nadir at resolution. SSR refers to the sampled subpoint resolution (SSR) at nadir due to over sampling in the east-west for GOES and north-south and east-west for Met-8/-9.

@ 15 min coverage 30 S northward
^ Met-8/-9 SEVIRI data is disseminated at 3 km resolution once the oversampled data have been remapped and georectified to a fixed navigation centered at 0°.
*Only available and disseminated at 4km.
In storage mode
& Backup to MTSAT-1R. Operational in 2010

active fire hotspot density it is important to keep in mind that a single GOES active fire hotspot pixel may reflect multiple MODIS detections due to the difference in spatial resolution (GOES at 4 km^2 versus MODIS at 1 km^2 at nadir). As is expected GOES and MODIS Aqua have similar fire prevalence patterns in the western hemisphere. Boreal fires peak in May-July, with mid latitude fires lagging 2 more months with peaks in summer (June-September northern hemisphere, or January Southern Hemisphere). In the sub- tropical Yucatán, northern South America, Equatorial Africa, and northern Southeast Asia (e.g., Thailand) fires peak in the February-May time frame. In August-October, overall burning peaks in Amazonia/Mato Grosso in South America, the savannah of Africa, and Indonesia and Northern Australia. Qualitatively, global/seasonal fire patterns are identical to other studies and well described in the literature [13], [20], [27], [28].

It has only been in the last two years that rigorous simultaneous characterization of GOES and MODIS fire products has been performed. A 50% detection threshold for active fire sizes of 500 m^2 and 1000 m^2 was found for MODIS and GOES respectively [23]. These detection efficiencies diverge for different fire regimes, which can cause sensors to report dissimilar patterns [23], [29].

An important example of this effect is the diurnal variability of fire, which peaks in the mid afternoon and is at a minimum near 3:00 AM local time. This diurnal cycle is largely a product of more rapid propagation of fire during the daytime peak of surface air temperature, but is also influenced by human practices in the case of agricultural and deforestation burning. The shape of the diurnal fire detection curve is robust for a wide range of ecosystem types [30]–[32]. MODIS overpasses on Aqua and Terra are near the diurnal peaks and minimums; however, the later afternoon overpass time of MODIS-Aqua results in roughly twice as many fire detections as Terra in the tropics. Because many fires will only burn actively during a fraction of the day, the WF_ABBA geostationary product, with its superior temporal sampling, detects twice as many fires overall in South and North America compared to MODIS. However, MODIS, with its superior spatial resolution and radiometric precision, detects 6–10 times as many fires in each

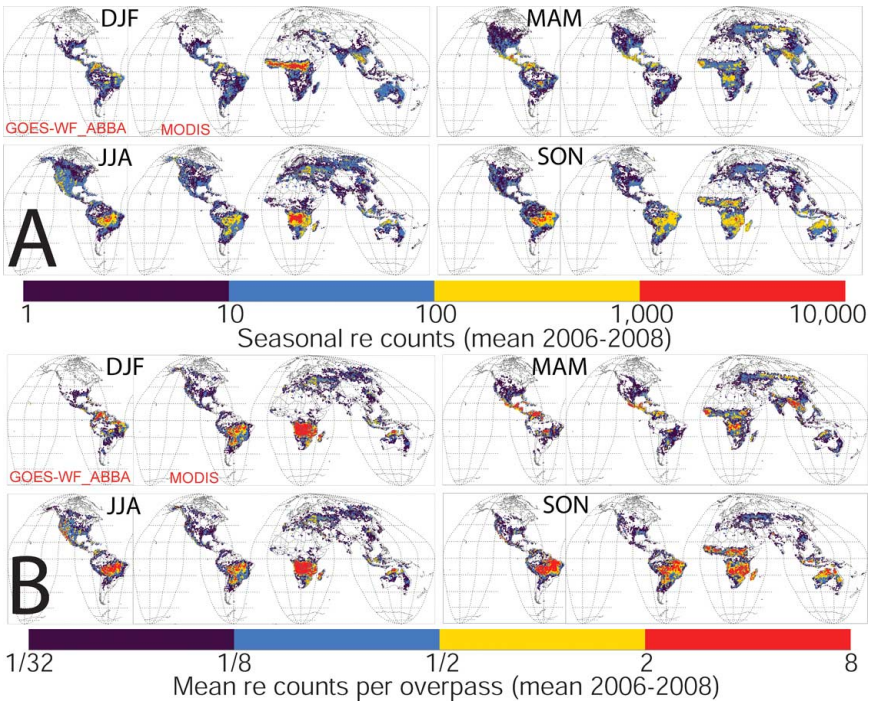

Fig. 1. GOES and MODIS fire (a) raw and (b) overpass normalized count statistics at 0.5×0.5 degree resolution for each season: DJF (December, January, February); MAM (March, April, May); JJA (June, July, August); SON (September, October, November).

overpass. The sampling advantage of WF_ABBA is reduced by the WF_ABBA temporal filter used to eliminate false alarms. Since the WF-ABBA processes as a serial stream, temporal filtering automatically screens the first fire detect of any fire. Consequently, small agricultural burns are also underestimated [e.g, compare detects in eastern United States-Fig. 1(b)].

Exact comparison of detection efficiency between the two instruments requires detailed information on blockout zones, view geometry, cloud filters, and other coverage gaps. Version 6.5 of the WF_ABBA product includes such metadata to facilitate a detailed evaluation of relative detection efficiency. Evaluation of absolute detection efficiency is limited by available validation data [33].

Despite the complimentary nature of the emerging geostationary and polar data, combining the two data sets into one unified highly quantitative product in a consistent and transparent manner is difficult. Fire detection and characterization has a number of nonlinear uncertainties with magnitudes that are sensor specific. These include: differing coverage schedules, variable pixel size based on viewing angle; pixel saturation temperature; differing spectral bandwidths; signal to noise issues; application of point spread function; diffraction; preprocessing chain including resampling and regridding; and navigational accuracy. A truly fused fire detection dataset requires a model of detection efficiency that takes into account not only these effects, but also interactions with different fire regimes. While progress has been made [20], [24], the development of an integrated approach is hindered by obtaining data suitable for validation. Given the rapid expansion of fire monitoring geostationary platforms considerable effort will be required to adequately characterize all sensors.

B. Source Function

The differences between individual fire hot spot data sources and qualities described in Section III-A as well as the uncertainty in establishing other emissions parameters leads to the viewpoint that fire data is semi-quantitative. Even so, source functions can include parameterizations that we consider to be "physically based" with the understanding that the complicated nature of the detection and emissions process dominates the uncertainty calculation. This consideration drives our rationale for the source function.

For the current FLAMBE source function, we exclusively use WF_ABBA GOES East and West fire products for the western hemisphere between 60°S and 60°N, and MODIS on both Terra and Aqua everywhere else. At high latitudes ($+/-60°$, demarcation) we sum WF_ABBA GOES and MODIS. It is expected within the next year, Meteosat and MTSAT-1R will be included in a new version of the source function. For each active fire hotspot, a net source injection is computed in a forward or "bookkeeping approach" [35]. For each model grid point

$$Flux = \sum_n m_{fn} \cdot f_{\mathrm{cn}} \cdot c_{fn} \langle EF \rangle_n \left(\frac{A_n}{T_n} \right) \tag{1}$$

where the biome/fuel specific intensive parameters are: $\mathrm{m_{fc}}$ -the amount of fuel mass available for combustion in kilograms per square meter; $\mathrm{f_{cn}}$ -the average mass fraction of carbon in the fuel; c_{fn} -the combustion factor (i.e., fraction of fuel that is combusted); and $\langle \mathrm{EF} \rangle_n$ –the fire average $\mathrm{PM}_{2.5}$ emission factor over the burn period in kg per kg carbon burned. Extensively, we need: A_n-the total area burned; and T_n- the average time between source function innovations (6 h for the global NAAPS,

TABLE II
INTENSIVE EMISSIONS PARAMETERS UTILIZED BY FLAMBE

Description	m_{fc}	f_{cn}	c_{fn}	$<EF>_n$	$PM_{2.5}$ Emissions (g m^{-2})
Bare/water	0	0	0	0	0
Light Grasses/tundra	0.2	0.5	0.6	17	0.85
Grasslands/Savannah	0.47	0.47	0.85	14	2.6
Cerrado/Woody Shrub	1.2	0.5	0.6	17	6.2
Crops	0.3	0.47	0.85	14	1.7
Temperate/Boreal-Low	10	0.51	0.5	32	82
Temperate-High	17.5	0.51	0.5	34	152
Tropical Forest	30	0.51	0.5	24	184
Wetland	1.7	0.5	0.6	17	8.7
Boundary regions	0.74	0.5	0.5	15	3.7
No data	0	0	0	0	0

m_{fc} -the amount of fuel mass available for combustion in kg m^{-2};
f_{cn} -the average mass fraction of carbon in the fuel;
c_{fn} -the combustion factor (i.e., fraction of fuel that is combusted);
$<EF>_n$ –the fire average $PM_{2.5}$ emission factor over the burn period in kg per kg carbon burned.

$<$ 1 h for mesoscale models). Thus, in this form, each active fire hotspot is given a total $PM_{2.5}$ emission in kg assigned to the model time step the active fire hotspot is observed.

To compute emissions, the fire location is mapped to a biome type from which all of the intensive parameters are derived. The USGS 1 km, 99 category AVHRR Global Land Cover Characterization version 2 database ([36]; http://edc2.usgs.gov/glcc/) is collapsed into 10 bulk categories: bare/water, light grasses, grasslands/savannah, low woody shrub and cerrado, crops, temperate and boreal forest-low fuel load, temperate forest-high fuel load, tropical forest, wetland, boundary regions. Intensive emissions parameters of (1) were derived from the literature ([14]; Table II). Of these parameters, ranking of relative average uncertainty to intensive parameters is $\sim 10\%$, 10%–30% and 20%–50% for the carbon fraction, combustion fraction and emission factors, respectively (see [14] for a full description of these uncertainties). Above ground fuel mass and fire area are highly uncertain, on the order of factors of 2 to 5 for any given fire, especially in areas of clearing where land use history can strongly affect available fuel [37].

Variability in emission factors results from a number of reasons and can be as large as an order of magnitude between fires in the same vegetation type; however, for fires in regions of heterogeneous land cover the simple Boolean comparisons of forest and nonforest are illustrative of baseline uncertainties [38]. In short, as seen in Table II, there is a factor of 10 to 100 difference in smoke particle emissions from light grass/semi arid to cerrado/savannah (~ 1 to 6 g m^{-2} burned) versus boreal, mid-latitude and tropical forest (~ 100 to ~ 150 to ~ 190 g m^{-2}). Consequently the key uncertainty in any emissions algorithm is derived from the ability to identify the relevant biome; everything else scales from this determination. Identification uncertainty is derived from the land use data base itself, unresolved sub-grid heterogeneity in land cover (manifested either as classification error for individual fires, or assignment to "mixed-class" categories in the land use product), changing landscape since the development of the databases (e.g., deforestation), and navigational uncertainty of the satellite data (e.g., on the arc of deforestation, a shift of less than one pixel can go from field to forest and, hence, a factor of 10 difference in emissions). The combination of these factors makes for a nonlinear uncertainty function where one field/savanna/cerrado fire misclassified as forest overwhelms the emissions of numerous other regional fires.

Once the intensive parameters are set, fire size is estimated. For WF_ABBA utilized fires, smoke fluxes are applied in the hour of the fire detection forming an hourly emissions product. We assume a fire moves through the entire area of the WF_ABBA derived sub-pixel fire size estimate per processed fire [hence, emissions rates in (1) is in kg per fire over the model time step]. For fires where size is not retrieved, a size of 50 ha is assumed for saturated active fire hotspots (the typical maximum for processed fires), and 5 ha for high-probability, medium-probability, and cloud-contaminated cases. Fires classified as a low-probability can represent the first detect for a new fire, but are often associated with false alarms and are ignored by FLAMBE emissions. For MODIS on Terra and Aqua, a diurnal correction is required to describe fire activity relative to local solar time per detection. Area burned for each MODIS fire-detection is estimated at 62.5 ha (relative to ~ 100 and 2500 ha MODIS pixel sizes at nadir and limb, respectively). This is distributed diurnally using a WF_ABBA based step function[30], [32] that releases 90% of total emissions between 0900 and 1900 local time. Differences between vegetation types are minor. Based on comparisons other analyses [31], the FLAMBE diurnal step function likely underestimates burning during the diurnal peak in most ecosystems, and may slightly overestimate nighttime emissions.

To assess the observability of biomass burning emissions, the original FLAMBE system simply forward modeled emissions, taking data products at face value as described above. However, we can expect a number of large offsetting uncertainties. We expect an underestimation of emissions due to undercounting of small fires from detection limitation for GOES (< 5 ha [33]), diurnal sampling or limb viewing for MODIS, or ground fires for both. Further subtract regional and sensor specific decreases in detections due to cloud coverage ($\sim 5 - 50\%$, [39]).

Converse to these potential underestimations, it has been found that even with an assumed "perfect" 120 m land cover database and perfect satellite navigation the sub-pixel forest/nonforest ambiguity from the 1 and 4 km nominal nadir pixel size from MODIS and GOES respectively can result in an emissions overestimate as large as 10% to 40% in mixed landscapes [38]. This does not account for navigation errors unrelated to resolution, or for variable pixel size across the limb, and is, thus, a lower bound for position error. Position-related biases in emissions could realistically be integer factors greater. We have chosen to stay with the supervised GLCC versus the unsupervised MODIS land cover database. Our studies show that using MODIS versus GLCC land cover results in regionally variable differences of a factor of 2 or more in emissions, with up to 50% lower global emissions using the MODIS product. But model validation has not shown improved error statistics using MODIS land cover. Therefore, in the interest of consistency, we have kept the GLCC database.

All of the above considerations demonstrate the challenge of comprehensive propagation of error when going from active fire hot spot observation to emissions to model validation. But, on a global scale in the presence of strong seasonal and regional burning covariance, much of the uncertainty appears to offset. Fig. 2 and Table III present seasonal emissions estimates for FLAMBE currently in use. A brief overview of re-

TABLE III
AVERAGE FLAMBE SMOKE PARTICLE EMISSIONS BY REGION AND SEASON OVER THE 2006–2008 TIME PERIOD

Region	DJF (Tg)	MAM (Tg)	JJA (Tg)	SAN (Tg)	Annual (Tg yr^{-1})	Annual With Regional Multiplier-Upper bound (Tg yr^{-1})	GFED 2006 Annual (Tg yr^{-1})
Sahelian Africa	6.3	2.8	2.1	0.7	10	x1.5 = ~15	9.8
Southern Africa	0.7	4.1	34	13	52	x0.5 =~26	9.7
Asia (East)	0.5	3.2	0.2	0.4	4.3	x2 = ~9	0.65
Australia	0.9	0.25	0.25	0.85	2.2	x2 = ~5	2.1
Boreal (North America)	0.003	0.015	0.15	0.004	0.2	x3= ~0.6	0.9
Boreal (Eurasian)	0.01	4.7	4.7	0.6	1.0	x3 = ~3	5.1
Central America	0.04	0.5	0.1	0.04	0.7	x3 = ~2	0.5
CONUS (Eastern)	0.02	0.12	0.13	0.04	0.3	X3 = ~0.9	0.3
CONUS (Western)	0.001	0.05	0.6	0.2	0.9	x2 = ~2	0.3
Europe/Mediterranean	0.03	0.1	0.7	0.1	1.0	x2 = ~2	0.3
Indian Subcontinent	0.1	0.6	0.03	0.03	0.8	x3 = ~2.5	5.9
South America	0.6	0.7	3.1	5.4	9.8	x3 = ~30	4.7
Southeast Asia (Insular)	0.3	1.1	1.3	1.9	4.6	X3 = ~12	8.2
Southeast Asia (Peninsular)	2.1	1.0	0.4	0.4	12.4	x1 = ~12	1.1
Global	12	28	46	24	110	x1.25= ~140	44

Included is the original emissions followed by a best estimate of a regional multiplier based on the ratio of free model versus data assimilation optical depths. Also shown in comparison is the GFED 2006 annual estimate. DJF (December, January February), MAM (March, April, may), JJA (June, July, August), SON (September, October, November). We consider the emissions with the regional multiplier as an upper bound of likely true emissions.

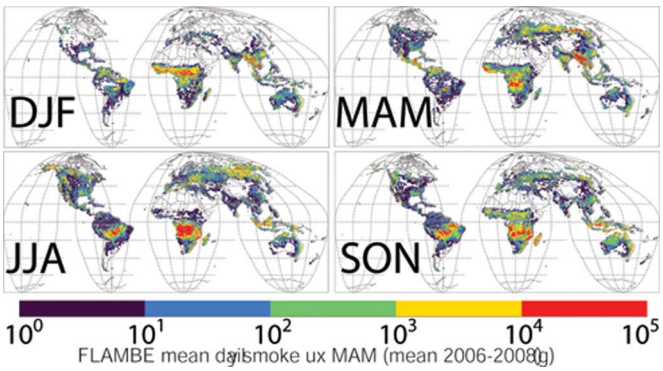

Fig. 2. Mean daily FLAMBE emissions in megagrams at 0.5 × 0.5 degree resolution at 0.5 × 0.5 degree resolution for each season: DJF (December, January February); MAM (March, April, May); JJA (June, July, August); SON (September, October, November).

gional emissions estimates in the 2006–2008 timeframe is presented here (Table III). Details of the nature of MODIS derived global fire patterns are well characterized [20]. As would be expected, emissions patterns are strongly correlated to the seasonal fire prevalence presented in Fig. 1. Globally, the original baseline FLAMBE emissions algorithm generated 110 Tg yr^{-1} of aerosol particles per year, associated with a total carbon emission of 4,700 Tg yr^{-1}. Consistent with other studies, the largest particle emitters are centered around the tropics, followed by Eurasian boreal and then mid-latitudes. In order of emission, we generated particle flux numbers of Central Africa (52 Tg yr^{-1}), Sahelian Africa (10 Tg yr^{-1}), Peninsular Southeast Asia (12 Tg yr^{-1}), South America (10 Tg yr^{-1}), Eurasian Boreal (10 Tg yr^{-1}), Australian (2 Tg yr^{-1}), Continental United States (1.2 Tg yr^{-1}), Europe and Mediterranean (1 Tg yr^{-1}), Central America (0.7 Tg yr^{-1}), Indian Subcontinent (0.7 Tg yr^{-1}), and North American Boreal (0.2 Tg yr^{-1}).

Transport studies using the original FLAMBE products showed that while optical depth and particulate matter correlations were very good against observations, there are persistent slope biases. Based on multiyear comparisons of NAAPS output to observations (some of which discussed in the next section), we are preparing to update the operational product to correct gross biases in regional aerosol loading. These empirical corrections will be applied regionally and seasonally (included in Table III). For example, in the western hemisphere where emissions are based on the WF_ABBA product, a factor of ~ 3 multiplier was required in order for the model to match observations of $PM_{2.5}$ and AOD in South America [13] and Central America [3]. The net effect of these offsetting modifications is a marginal increase in global smoke emissions of roughly 25%.

C. Transport Modeling

A unifying thread for all of the smoke forecasting work is the NAAPS global aerosol model run operationally at the Fleet Numerical Meteorological and Oceanography Center (FNMOC). NAAPS is a modified form of a hemispheric sulfate chemistry model [40]. NAAPS uses global meteorological analysis and forecast fields from the Navy's 0.5° × 0.5° Operational Global Analysis and Prediction System (NOGAPS, [41], [42]) on a 1° × 1° global grid at 24 vertical levels reaching 100 hPa. Dust, sea salt, and, for FLAMBE, smoke has been added to the original model [13], [43], [44]. NAAPS is being upgraded to 0.5° × 0.5° resolution and 42 levels. Four times daily, the NOGAPS weather forecast model provides dynamical and surface fields to the NAAPS at 6-hour intervals for a six-day forecast period. Transport is calculated using a 5th order Lagrange scheme [45] with calculated departure points [46] while horizontal and vertical diffusion are calculated with a finite element scheme.

Aerosol microphysics in NAAPS is relatively simple. This is in response to the needs of a forecast model to be computationally fast, its operational requirements (e.g., forecast severe visibility reducing events) and the fact that in comparison to the uncertainties in source functions as well as transport meteorology, microphysics is relatively well constrained. The primary aerosol

quantity in NAAPS is optically active aerosol mass. Size distributions are not explicitly modeled, nor are secondary particle production mechanisms, except for SO_2 and sulfate.

Smoke is injected into NAAPS as a well mixed plume in the boundary layer, a reasonable estimation for fires in the tropics and subtropics where smoke is capped by the subtropical subsidence inversion [47], [48]. For large boreal complexes, typically smoke peaks at the top of the boundary layer inversion which is typically around 0.7–2 km [49]. By performing a mixture coupled with numerical diffusion we are making a zero order correction for the $\sim 20\%$ that makes it above the boundary layer. Further, long periods of smoldering and surface peat and duff fires also make this a reasonable approximation. Given the smoke is well mixed in the boundary layer, within a single global model grid point smoke should be mixed relatively quickly. Hence, as a sub pixel parameterization, we perform this mixing during the initial injection.

After injection the coagulating plumes rapidly photochemically evolve, thus typically increasing particle mass by 10%–50%, with some laboratory studies suggesting integer factors more [14], [47], [50]. Both of these aspects are highly nonlinear, and model resolution significantly impacts solutions. We consider these aging effects as part of the uncertainty of the source function itself and include them in the regional corrections given later in the paper. Particle microphysical and optical parameters are drawn from the compilations presented in [47], [51]. The dry mass scattering and extinction efficiencies are taken as 4.3 and 4.7 m^2g^{-1}, respectively ($\omega_o = 0.91$ at 550 nm). These numbers are probably on the order of 10%–20% low for the largest temperate forest fires, and $\sim 10\%$ high for grass/savanna type fires. The asymmetry parameter is assigned as 0.6 ($+0.04$ uncertainty). The hygroscopic growth function is taken from studies in Brazil [52]. An error analysis suggests that at 80% RH, this yields another 15% uncertainty in light extinction [51]. Given the significant uncertainty in the source function alone, all of these uncertainties are small. Findings on transport and smoke coverage from the NAAPS model are presented in Section IV.

In addition to the global model, FLAMBE has also been run in mesoscale simulations. In a baseline mode similar to NAAPS, FLAMBE source functions have been utilized for field campaigns and severe domestic burning events using the operational US Navy Coupled Ocean/Atmosphere Mesoscale Prediction System–On Scene (COAMPS-OS®,[1] [53]). COAMPS-OS® is a turnkey mesoscale model built around the research and operations version 3.0 of COAMPS® [54]. COAMPS-OS® is also operationally run at FNMOC, and used by NRL scientists for basic research. COAMPS® is nonhydrostatic, compressible, and includes explicit cloud microphysics. COAMPS-OS® model boundary conditions are provided from the operational $0.5^\circ \times 0.5^\circ$ NOGAPS runs. Mesoscale data assimilation is performed at 12-h incremental update cycles also using NOGAPS and assimilated data therein.

While COAMPS-OS® is used in an intermittent forecasting capacity, for mesoscale research FLAMBE was incorporated into the Regional Atmospheric Modeling System (RAMS)-Assimilation and Radiation Online Modeling of Aerosols (RAMS-AROMA, [3], [55]). Based on the Colorado State RAMS mesoscale model, RAMS-AROMA was used to examine the transition of FLAMBE from a global model to the mesoscale. Studies included top-down estimates of the smoke emission uncertainty at higher resolution and the quantification of smoke radiative forcing and meteorological feedbacks in regional scales. Similar to COAMPS®, RAMS was developed as a mesoscale meteorological model that numerically solves nonhydrostatic atmospheric equations [56] and has been successfully used to simulate a wide range of atmospheric phenomenon including sea breezes, severe storms, flash flooding, downslope winds, air pollution and atmospheric convection ranging from boundary layer (large-eddy) cumulus to mesoscale convective systems [57]. RAMS-AROMA was built upon RAMS by adding the following new features and modules: (a) an aerosol transport model that includes the aerosol emission, advection, convection (vertical motion), dry and wet deposition processes [3]; (b) a delta-four stream model [58] to better treat the impacts of both clouds and aerosols on the radiative transfer [3], [59]; and (c) an assimilation package that can assimilate the satellite-derived aerosol optical thickness [59] and (d) a smoke emission module [3] for improving the model initial and boundary conditions of aerosols. With the above design, the aerosol radiative impacts in RAMS-AROMA are directly tied into the simulated physical processes in the atmosphere, allowing the dynamical processes in the model to impact aerosol transport and vice versa. Findings for RAMS-AROMA are also presented in Section IV.

D. Remote Sensing and Data Assimilation

The FLAMBE program was originally intended to be integrated with remote sensing data. Until recently, this integration has been on the semi-quantitative level. In this way, FLAMBE fire observations and emissions estimates have been used in conjunction with NAAPS and RAMS-AROMA output fields to interpret remote sensing data from MODIS, MISR, CERES and AERONET. These comparisons were used to constrain smoke emissions [3], [13], radiative forcing [59], [61], and transport [1], [5].

A new quantitative phase of FLAMBE has begun with the development of data assimilation systems. MODIS data collection 5 aerosol AOD assimilation is being transitioned to operations via the Naval Variational Analysis Data Assimilation-Aerosol Optical Depth system (NAVDAS-AOD; [62]). Through a series of quality assurance and empirical corrections of original MODIS level 2 over ocean aerosol products [63], a new data assimilation quality level 3 product has been generated [64]. For over ocean, assimilation is based on the NAVDAS-AOD 2-D var scheme for sulfate, smoke and dust. Sea salt is sufficiently small in optical depth relative to MODIS uncertainties it is not impacted by assimilation. Fine and coarse mode optical depth speciation resides with the model background field. For ocean and coastal sites this has reduced NAAPS AOD bias against AERONET by 50% over a 48 hour forecast period [62].

Over land, the situation is much more complicated. Because of the more complex lower boundary condition with an accompanying reduction in signal to noise, error functions for over land products are considerably more complicated. Over land MODIS data is currently being added to the level 3 product.

[1]COAMPS® and COAMPS-OS® are registered trademarks of the Naval Research Laboratory

While this is not fully developed, as an example we use the original MODIS product for over dark land regions and include the results in our findings presented here (Section IV). However, these assimilation runs are based on the natural MODIS AOD products [65] without bias elimination as done in the over water case. Hence, any systematic errors in the MODIS products will manifest themselves in the validation statistics. These biases are regionally specific due to the tuning performed during product development [65]. Even though data assimilation methods are still in development, we include them in this paper and analysis to demonstrate the improvement such methods can provide.

E. Data Distribution and Validation

All FLAMBE products are considered part of the public domain. Operational geostationary fire products are available from NOAA NESDIS. Quasi-operational geostationary WF_ABBA products as well as source functions are available on the NRL Aerosol (http://www.nrlmry.navy.mil/aerosol/) and FLAMBE websites (http://www.nrlmry.navy.mil/flambe/) which distributes roughly 1 Gb of data per month. Model data can be found at the Global Ocean Data Assimilation Experiment server (http://www.usgodae.org/links.html).

FLAMBE has a series of automated validation products. On-line, FLAMBE users can view running 2 week comparisons of modeled versus Aerosol Robotic Network (AERONET) observed AOD at the NRL aerosol website [66]. Similarly, daily comparisons of modeled versus MODIS AOT is also available on the same site. In this paper, we present validation statistics based on AERONET at the instantaneous and 7-day average level.

IV. Findings and Validation of Global Biomass Burning Phenomenology

Biomass burning smoke has far reaching effects, with intercontinental transport a fairly common occurrence. In this section we give an overview of FLAMBE results and performance based on comparisons to AERONET level 2 data, or when not available, through the MODIS data assimilation innovations. We do not have an adequate source of consistent global vertical information, although a new CALIPSO product is being developed for comparison to the model and eventual assimilation [67].

Table IV contains regressions of FLAMBE smoke AOD to fine mode optical depths as derived from a spectral deconvolution method [68]. Sites in Table IV were selected due to the high fraction of fine model optical depth and smoke prevalence as well as a lack of other aerosol species such as dust or pollution. Evaluation is based on a 2006 and 2007 NAAPS run with and without MODIS data assimilation [62]. Fig. 3 presents seasonal average aerosol optical depths from the FLAMBE system for one year (December 2006 through November 2007). Fig. 3(a)–(d) shows AODs using the original FLAMBE source function, with Fig. 3(e)–(h) using MODIS AOD data assimilation. Here we only present FLAMBE analyses and save the forecast validation for a separate paper.

The dominant transport patterns associated with burning are fairly clear for tropical to subtropical regions. Smoke from Africa and South America feed into the South Subtropical Atlantic and southern mid-latitudes. Smoke from equatorial

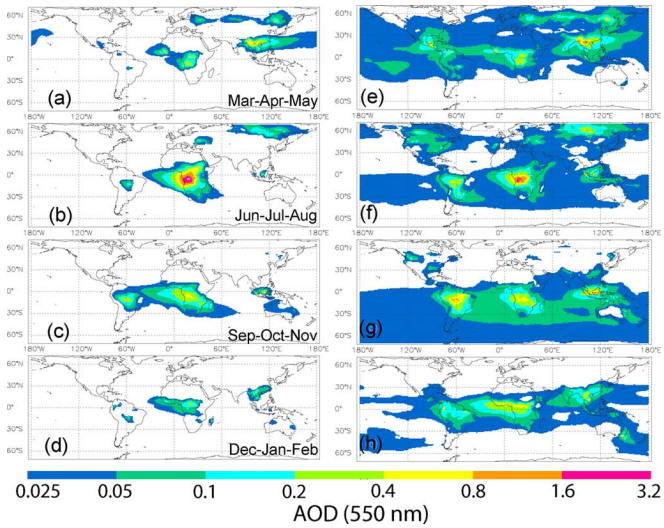

Fig. 3. FLAMBE/NAAPS seasonal optical depths (550 nm) from the natural run using the baseline FLAMBE emissions product (a)–(d) and MODIS AOT data assimilation (e)–(h).

Africa is transported in the easterly trades across the tropical Atlantic. Spring time emissions from Central America and Asia transport simultaneously into the United States. The inclusion of data assimilation altered the magnitude of optical depth, but did not much change the patterns of smoke coverage. Significant increases in smoke AOD were found over South America, Central America, Equatorial Africa, Southeast Asia and the Eurasian Boreal, as was an increase in smoke activity in Southeastern Australia. Decreases in AOD were only found in central and southern Africa. Data assimilation also brought the background optical depth to just cover the 0.025 plotting threshold in the key oceanic receptor regions of the globe-northern hemisphere in spring, southern hemisphere in summer and fall, and tropics in winter.

A detailed discussion on each of the emissions and transport pathways over the globe exceeds the scope of this paper. However, in the following subsections, we will discuss key global scale emissions and transport properties with appropriate AERONET validation statistics. To reiterate, FLAMBE has operational and scientific objectives. From an operational point of view, we want FLAMBE to predict the onset and transport of large smoke events, nominally relative indicators clean, moderate and severe with trends (i.e., variance) out weighing amplitude. Scientifically, we are interested in the observability problem. Namely, how much of the variance can we capture with the simplest possible model, with the fewest empirical parameterizations?

A. Southern Hemisphere Atlantic: South America and Africa

South America and Africa account for over ½ of the smoke fluxes in FLAMBE, FLAMBE data assimilation adjusted, and the independent GFED databases [27]. South America was the first continent extensively studied in the FLAMBE system and South America is where FLAMBE performs best. Over the 2006–2007 validation timeframe here, results and performance were identical to early system results [13]. In summary of this earlier work, FLAMBE correctly placed the seasonality of South American burning (August-November along the arc of

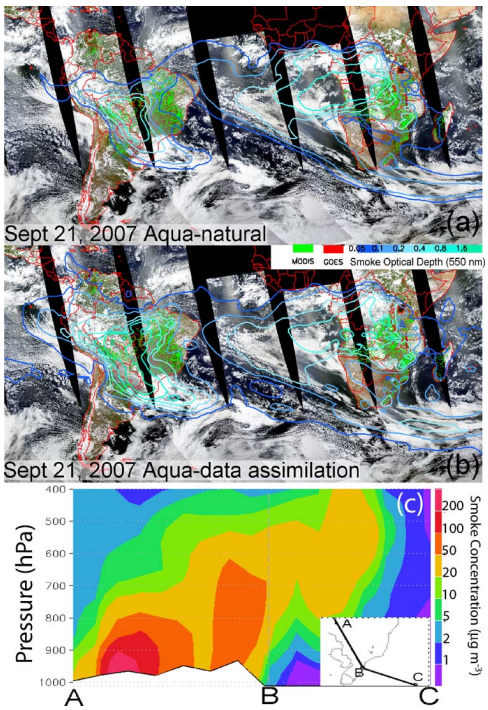

Fig. 4. GOES (red) and MODIS Aqua (green) active fire hotspots and NAAPS 550-nm smoke optical depths overlaid on MODIS Aqua RGB for the South America and Africa transport event of September 21, 2007. Included are optical depths from the (a) natural and (b) optical depth data assimilation runs. (c) Cross section of South American smoke along the center of the plume from Amazonia into the South Atlantic Ocean.

deforestation in Brazil and Bolivia; Venezuela and Colombia in February-March). Without data assimilation, correlations for AOD against AERONET at three key receptor sites in Brazil (Alta Floresta, Cuiaba, and Rio Branco) are greater than 0.75, and 7-day correlations are on the order of 0.85–0.95 (Table IV), capturing more than half of the variance of the smoke AOD. With data assimilation, correlations range from 0.84–0.95 and 0.72–0.99 for the instantaneous and 7 day, respectively. Such high correlations are not unexpected, as burning is spatially correlated across South America.

The comparison against AERONET also reveals two consistent findings. First, as previously reported [13] natural modeled AODs for FLAMBE for 2001 were low by $\sim 50-70\%$. Second, the data assimilation shows that remote sensing bias directly impacts the simulation. MODIS on Aqua has shown a 60% high bias relative to AERONET in South America. This bias is directly reflected in the DA modeled slope against AERONET. Further, while in general DA improves correlations, there may still be cloud bias in the system adding noise. For Rio Branco, DA reduced correlations, a result of a few data points far off the regression line due to cloud contamination in the vicinity.

As in South America, fire activity in Africa is highly correlated spatially and seasonally. A central plume is visible over most of the year and typically caught in the easterly trade winds and transported over the South Atlantic Ocean and as far west as South America [69]. Burning is prevalent in the Sahelian region starting in the spring, and moves south to Southern Africa in the June timeframe. The Sahel also has a secondary burning peak in the fall. The majority of the burning, however, is in southern Africa around Congo and Zambia with a peak in the August timeframe.

Natural FLAMBE performance in central Africa is also good near the source ($r = 0.5 - 0.7$ for instantaneous and 7-day). In addition to the large differences in fire regime between the area and South America, the data inputs to FLAMBE are also different (MODIS fire in Africa as opposed to WF_ABBA in South America). Opposite to South America, biases near the source in central Africa are 50% high. This is also corrected in the DA run, where correlations and slopes also vastly improve-although, MODIS here has a 15% low bias. At the Ascension Island receptor site over the Atlantic, correlations are low, but so are mean optical depths (< 0.1). For equatorial Africa, natural and DA performance is less than to the south, with instantaneous and 7 day correlations around ~ 0.3, and 50% low biases. DA dramatically increases the slope to 0.73-0.84 and correlations to 0.61-0.72 and 0.83-0.87 for instantaneous and 7 day data points.

Long range transport from South America and Africa appears to be reasonably coupled. First, seasonal particle production are in phase, with Central Africa peaking perhaps one month before South America in the August timeframe. Transport in both burning regions is influenced by the so called South African Gyre [70] or in meteorological fields the South Atlantic Subtropical High (SASH). A typical regional example of smoke fields for September 21, 2007 is shown in Fig. 4 with data assimilation (the free running model is identical in shape, but with positive and negative biases in AOD for Africa and South America, respectively). Also shown is a height cross-section along the plume center from Amazonia out over the Atlantic [Fig. 4(c)].

As smoke builds up in Amazonia it is transported south along the Andes Mountains by the SASH and eventually advected along cold fronts into the Southern Atlantic Ocean [13], [15]. Smoke is typically capped by the 700 mb subsidence inversion. However, as it is transported south it is synoptically lifted along lines of constant potential temperature and eventually becoming an elevated plume [Fig. 4(c)]. Since these cold fronts have significant cloud shields, this transport phenomenon is difficult to observe by satellite; [13], [71].

African smoke is transported westward by easterly winds, crossing the coast over Namibia. While a portion can continue on to South America (e.g., *Anderson et al.*, 1996), the majority wraps around the SASH in what is frequently referred colloquially as the "South African river of smoke." From there smoke moves into the southern storm track, ultimately transported along a path to Australia. As in all cases of subtropical transport to higher latitudes such as Fig. 4(c), smoke becomes elevated. In this case, smoke was advected in the southern westerlies at the 600–400 hPa range ($\sim 5 - 7$ km).

What is interesting is the relative coherence of the African and South American transport around the SASH and into the storm track. Fig. 4 presents a case of parallel transport. This appears to be most often associated with wave number 5 features over the southern ocean and occurs $\sim 10 - 15$ times per year.

B. Boreal Smoke Production and Transport

Next to South American fire monitoring, boreal fire monitoring has been the second most commonly utilized part of FLAMBE. FLAMBE is regularly used in both forecasting and

TABLE IV
KEY VALIDATION SITE REGRESSIONS FOR 550 NM FLAMBE-NAAPS MODEL RUNS AGAINST AERONET

Region	#Points	Instantaneous Natural	Instantaneous DA	7-Day Natural	7-Day DA
Africa (Above Equator)					
Djougou (9.8 N; 1.6 E)	11466/69	0.41/-0.04/0.28	0.84/-0.025/0.61	0.13/0.01/0.36	0.73/-0.02/0.83
Ilorin (8.3 N; 4.3 E)*	11207/100	0.42/-0.07/0.33	0.77/-0.05/0.72	0.1/0.04/0.2	0.73/-0.03/0.87
Africa (Below Equator)					
Ascension Island (8.0 S; 14.4 W)	3188/19	0.60/0/0.22	0.82/0.02/0.71	0.03/0.02/0.01	0.5/0.04/0.76
Mongu (15.2 N; 23.2 E)	10318/67	1.7/-0.1/0.51	0.85/0.03/0.91	0.837/-0.02/0.73	0.839/0.01/0.95
Boreal (North America)					
Bratt's Lake (50.3 N; 104.7 W)	19366/30	0.1/0/0.49	1.0/-0.02/0.78	0.08/0/0.52	0.86/-0.01/0.89
Bonanza Creek (64.7 N; 148.3 W)	4063/42	0.37/-0.01/0.26	1.3/-0.04/0.52	0.12/0/0.4	0.88/-0.02/0.76
South America					
Alta Floresta (9.9 S; 56.1 W)	9952/39	0.56/0.01/0.75	1.2/-0.03/0.84	0.39/0.03/0.89	1.1/0.04/0.97
Cuiaba (15.7 S; 56.02 W)*	8213/81	0.4/0.02/0.75	1.6/-0.06/0.98	0.41/0.03/0.85	1.5/-0.05/0.99
Rio Branco (10.0 S; 67.9 W)	4902/32	0.46/0.01/0.83	1.6/-0.07/0.85	0.50/-0.01/0.96	1.6/-0.03/0.72
Southeast Asia (Insular)					
Silpakorn (13.8 N; 100.0 E)	2747/29	0.49/-0.08/0.47	0.89/-0.05/0.71	0.33/-0.03/0.70	0.91/-0.05/0.0.87
Pimai (15.2 N; 102.6 E)	10205/77	0.47/-0.05/0.72	0.90/-0.05/0.83	0.3/-0.02/0.73	0.69/-0.01/0.80

Data is for smoke dominated regions for the years 2006- 2007 (Slope/Y Intercept/Correlation coefficient). Regressions are for NAAPS smoke optical depth versus fine mode optical depth derived from the O'Neill spectral convolution method. Background aerosol concentrations for these sites were less than a quarter of the perceived smoke signal.

research circles to monitor the production and transport of boreal smoke, particularly Alaskan and Asian smoke to the continental United States and beyond [1], [5], [28], [72], [73]. Eurasian and Siberian boreal forest fire activity concentrates around the 50–60°N latitude range. This forested region is far enough north so that it has not been converted to agriculture, but not so far north that the biome has transitioned to tundra. Studies using FLAMBE data show that not only does Siberia impact west coast air quality [1], but because of high latitudes of emissions, transport over long distances is favored and Siberian smoke is being observed as far east as the Azores [5].

The monitoring of northern latitude North America burning pushes the geostationary products to its limits and consequently biases and correlations are lower than in the tropics. Low biases for North America in the Bratt's Lake and Bononza Creek AERONET stations are on the order of 80% with correlations ranging from 0.26–0.49 and 0.4–0.52 for instantaneous and 7 day averages, respectively. This is because the high latitudes increase of the geostationary pixel size coupled with topographic shading produces a smoke product that is low by a factor of two to four. In the case of the Quebec wildfires of 2002, at latitude of roughly 52N, FLAMBE emissions were estimated to be too low by a factor of two [72]. For Alaska the years 2004 and 2005 showed very intense burning in Alaska ($>$ 8 Mha, 10% of boreal land burned, 60N-70N latitude). Correlations were better, but predicted optical depths were low by over a factor of 4, certainly due to the very high latitude of these events and WF_ABBA processing limits in this region. DA vastly improves performance, nearly removing bias and increasing correlations to 0.52-0.78 and 0.76-0.89 for instantaneous and 7 day averages, respectively.

Because of other major aerosol species such as dust and pollution, there are not any good AERONET stations in Asia for validation which can easily isolate biomass burning smoke. Based on the innovation vectors ($\sim$ factor of $1.25 - 2$) for DA, we believe performance is better than the natural runs. This is most certainly due to the use of MODIS fire products, which not only have better resolution than GOES, but also more frequent coverage over the higher latitudes than the tropics. Fig. 5 demonstrates a case of peak burning in Siberia in May 2007. Smoke is transported behind frontal systems and transported over the Pacific Ocean and on occasion, Alaska and North America [1]. In this particular case, the smoke band was transported across the Atlantic at the 500 hPa level ($\sim 5-6$ km). Like most other cases, DA increases smoke AOD. Of note is the increase in smoke AOD in the mid-Pacific, which coincides with a darkening of the clouds in the image. This demonstrates how DA over land can have a lasting impact in the model forecast.

C. Southeast Asia

Fire prevalence is significant in Southeast Asia, but except for case studies during the massive events, it is to a large degree unstudied systematically. SE Asia is a particularly difficult area to perform biomass burning research. High cloud cover fractions (both convective and cirrus) frequently mask fires and smoke. Total emissions from the region are small in comparison to Africa and South America, but burning emissions per unit area in the FLAMBE algorithm are on par if not greater than

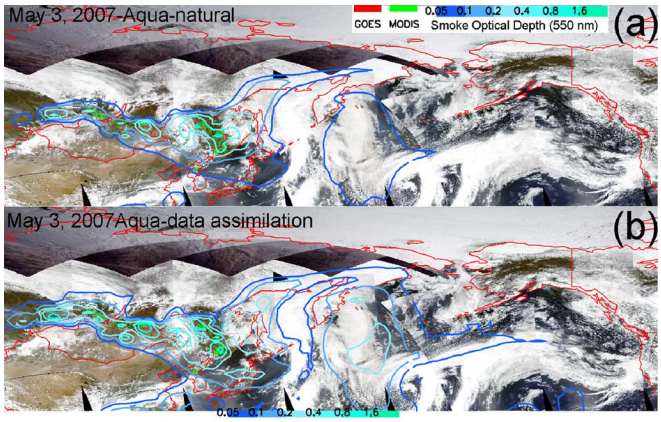

Fig. 5. Same as Fig. 4, except for the Siberian boreal fire of May 3, 2007.

these other burning regions. While there is a definite seasonal signal, unlike Africa and South America, burning events also exhibit strong interannual variation. Some of the more famous episodes include El Nino events in 1997 and 2002 when very thick smoke covered the region for months. From Figs. 1–3, it is evident that there are two key burning seasons in SE Asia. In the December–April time frame when the ITCZ is at its most southern extent, significant burning occurs in Peninsular SE Asia, particularly in Thailand, Cambodia and Burma. If conditions are sufficiently dry, burning can extend as far south as Northern Sumatra and Indonesia. FLAMBE correlations here are reasonable, with the Silipakorn University and Pinai AERONET sites located in the middle of the burning region having natural correlations of 0.47–0.72 and 0.70–0.73 for instantaneous and 7 day averages respectively. Like many parts of the world, a factor of 2 low bias is evident. DA improves the analysis, increasing correlations to 0.71–0.83 and 0.87–0.8 for instantaneous and 7 day, respectively, with slopes on the order of 0.7 to 0.9.

During the northern phase of the ITCZ (May-October), significant southern burning begins on Java, Sumatra and Borneo, with some additional burning of the Malay Peninsula. Peak burning tends to occur in the September-October time frame, but with March-May events not being uncommon. The only AERONET data in this region is Singapore, where extraction of the biomass burning signal has been difficult due to many other local pollutants and persistent cloud cover. When MODIS AOD data are available, innovation vectors suggest that perhaps as much as a factor of 4 increase is required, which is similar to results of comparison to surface $PM_{2.5}$ observations in Malaysia [74].

Transport in SE Asia tends to be to the northeast all year round, with occasional intrusions into the Bay of Bengal in the September-October timeframe. In the southern burning phase, smoke coverage tends to be limited with advection into the ITCZ predominately in the South China Sea. The northern phase, however, appears to have much more significant coverage. Fig. 6 demonstrates such a case of burning in Thailand and Cambodia that advects to the northeast over Taiwan and into a westerly wind region just south of the Pacific storm track. Long range transport was modeled to be at the 500 hPa ($\sim 5-6$ km) level. The natural run has a stronger plume signal than with DA, but the general pattern is the same. These types of events appear annually in the model. Although AOD enhancement is small on the west coast of the United States, this shows the large geographic range that SE Asian smoke can advect, and larger enhancements for more persistent pollutants might be expected.

D. Central America

Because of air quality [3] and potential meteorological impact [11], [12], smoke in the southeastern United States (SEUS) is of special interest. In the March-May timeframe each year, FLAMBE monitors smoke from the Yucatan Peninsula being transported into the SEUS (Figs. 3 and 7). Due in part to the short season and the lack of sites, there are no available AERONET sites for a credible annual analysis. But DA suggests that, like South America, a factor of two low bias in optical depth is present in the NAAPS simulation.

There has yet to be a complete analysis of Central American smoke with the global NAAPS model, but the region has been studied extensively at the mesoscale. During the spring of 2003, the Central American region was unusually dry, causing a significant increase in emissions [75]. Under the influence of southerly winds, smoke crossed over the Gulf of Mexico and intruded deep into the SEUS. FLAMBE emissions for this season were examined using a mesoscale transport model based on RAMS [3], and all of the findings appear to hold for the global NAAPS model. In agreement with the global model analysis, RAMS-AROMA showed that the baseline emissions model was low for both AOD and $PM_{2.5}$ by about a factor $\sim 2-3$ [Fig. 7(c)]. This seems to be typical interannually.

By using FLAMBE emissions in the much higher resolution RAMS-AROMA model, additional experiments were performed to examine how FLAMBE can be ported to the mesoscale. We found that: (a) the injection height of tropical biomass burning aerosols can be approximated as in the boundary layer with a resultant $\sim \pm 20\%$ uncertainty in the simulated smoke particle concentration; (b) the diurnal variation (and, hence, the need of using hourly) of smoke emissions is important for the modeling of smoke distribution in the smoke source region but not in the downwind hundreds of miles away [3]; and (c) through radiative heating in the atmosphere and radiative cooling near the surface, smoke particles increase the lower-tropospheric stability, which sometimes may couple with the middle-to-upper tropospheric convection [Fig. 5(a)], producing feedbacks on dynamics and cloud microphysics with important implications for the forecasts of air quality and weather [12], [60].

E. Continental United States and Europe

Last, we would like to address fires from continental mid-latitude forest and agricultural fires in the United States and Europe. These regions pose the largest challenge to fire monitoring and smoke prediction systems. There are a number of factors that make this region distinct. Fuel load, combustion fraction, and emission factors are much more uncertain for temperate forest and scrub regions, and fire intensity becomes a key term in emissions estimation [14]. Whereas in most tropical areas burning is more seasonal and occurs over large areas, burning in the US and Europe is much more sporadic. Hence, unlike the tropics and subtropics where burning activity in whole regions co-vary

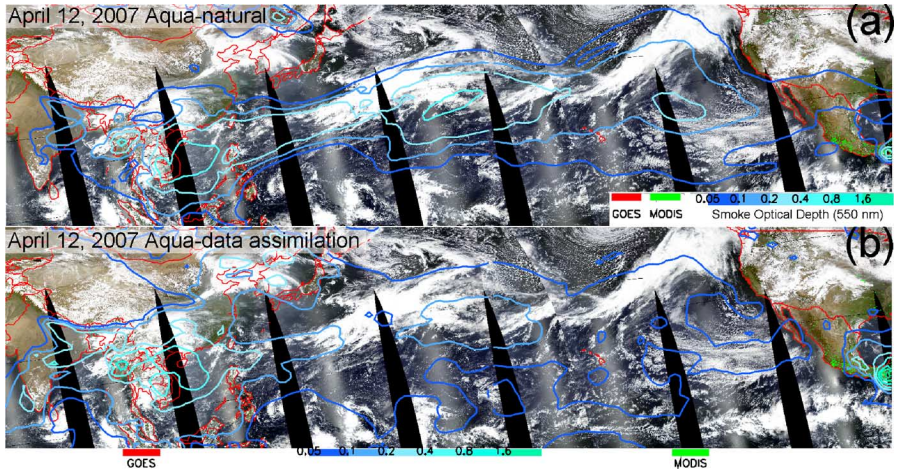

Fig. 6. Same as Fig. 4, except for the SE Asia fire plume of April 12, 2007.

and a bulk source function is adequate, for an individual temperate forest fire there is no compensation of error to help offset the uncertainties of the individual source terms. In cases where there is intercontinental transport and impact in western countries, the transport length scale is much larger than the source region scale. But, for fires within western countries, individual fire plumes are important and impacts need to be characterized within the first 100 km.

Detection and emissions modeling of agricultural fires and smaller wildfires is particularly difficult. Agricultural fires are very short in duration and are often not captured in MODIS, and temporal filtering may lose many even with WF_ABBA. Also for agriculture, there is often not an easily available database as to what material is burning (e.g., grain stubble, range etc, [76]). For smaller fires, agricultural burning, or even isolated large fires, there is a lack of validation data.

Last, we must consider that the end user for air quality applications in temperate zones is much more demanding. Whereas individual transport events into the region are clearly visible in the models and thus individual violations can be attributed to a single event, the more frequent background fires are more difficult to characterize.

FLAMBE was not originally designed to deal adequately with the mid-latitude meso-scale problem. Even so, as part of the system fires and emissions are processed with the rest of the system. For most agricultural burning, smoke appears to rapidly diffuse into the continental background. For large fires, FLAMBE captures the basic transport patters and appears to correlate well with what data is available. Operational CONUS fire emissions are a focus of active development in the NOAA NESDIS program [32], [77], [78].

V. Discussion

There is a great deal that we have learned about the nature of global biomass burning through the FLAMBE system which is both encouraging and humbling. Clearly, even from a pure forward model the bulk of biomass burning emissions and smoke coverage can be simulated with reasonable correlation at even the instantaneous level. With improvements that AOD DA brings, we have even higher confidence in smoke coverage and subsequently forecasting. For the primary purposes of the FLAMBE system, this is largely sufficient. Yet even a cursory error propagation of the forward models demonstrates that we have very far to go in isolating individual components of the biomass burning system. In this section we wish to discuss two key topics: total particle emissions and a roadmap for future development.

A. Emissions

In our forward model, near-real-time fire detection data are used to estimate "true" fire burned area. From the fire location data, the ecosystem is identified and fuel load estimated. Fire intensive properties such as combustion fraction, intensity, and emission factors are all intertwined, as is time of burning: agricultural fires present a detection problem as they may burn for only a short time ($< 1-3$ h), whereas peat fires in boreal regions and in SE Asia are capable of burning for days. Then there are uncertainties of injection, transport, evolution and scavenging. To tie the model to observables, optical properties need to be computed and integrated. Last, validation data sets cannot necessarily be taken as "true" and have their own sets of measurement and sampling biases. True propagation of error for any individual fire is daunting.

For the globally significant burning regions, however, spatial and intensive burning properties covary and through compensation of errors we can derive a reasonable representation of smoke coverage. In tropical fire regions, in particular with large regionally coherent burning patterns, uncertainties due to random error assignments of say fire size or even detection probability are reduced. Even though strong nonlinear biases exist in regions along arcs of deforestation due navigational/eco system assignment errors (such as Amazonia [38]), South America is where FLAMBE performs best. Indeed, it could even be argued that given the uncertainties in establishing emissions from individual fires, for regions of high fire activity all that may really be required is the relative number of fire count (such as being developed for NASA GEOS 5) or even a relative low, medium, or high emissions scale. These gross simplifications of course become less true as fires become more sporadic, with individual mid-latitude fires being the most difficult to characterize.

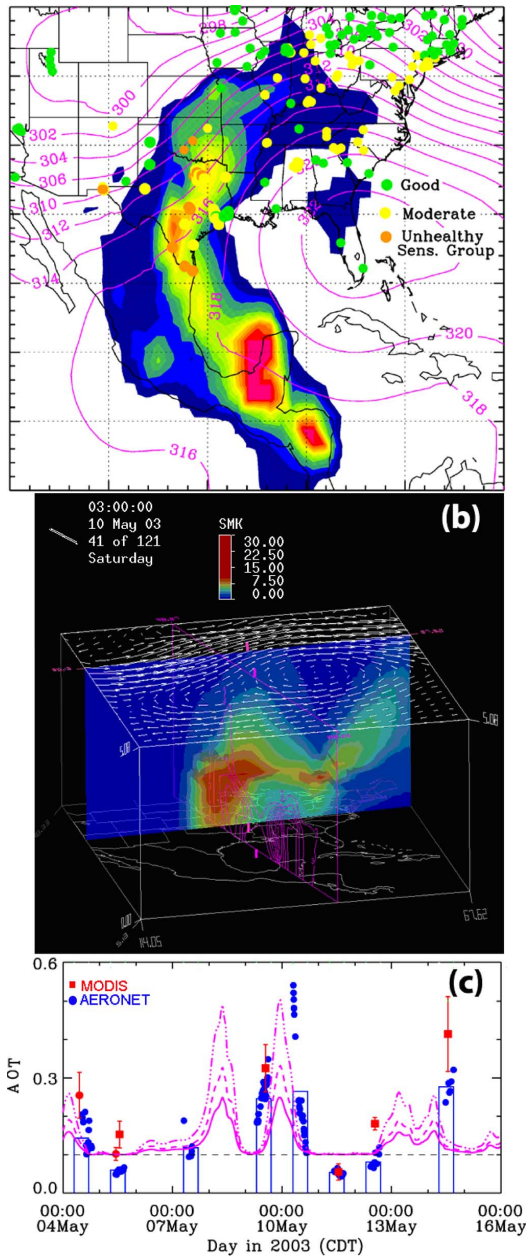

Fig. 7. (a) RAMS-AROMA simulated smoke mass distribution on May 10, 2003, showing smoke transported northward from the Yucatan Peninsula to Texas and then northeastward over the Great Plains to the southeastern U.S. (b) Similar to (a) but shows the vertical slices of smoke mass concentration respectively in the north-south direction (pink-color contour lines) and east-west direction (filled-color contour), indicating that smoke particles were trapped in the boundary layer before they were uplifted over the Great Plain by the trough that can be identified from the 500 mb wind vector (shown as white arrows on the top of 3-D box). (c) Time series (in CDT, Central Daylight Time) of aerosol optical depth (AOD) at the ARM SGP site derived from AERONET (blue dots), MODIS/Terra (red dots), MODIS/Aqua (red squares), and RAMS-AROMA simulations (pink lines), respectively, using FLAMBE emission inventory (2002 version) with no change (solid pink), 50% increase (dash pink), and factor of 2 increase (dot pink). The MODIS AOT values and their error bars are reported, respectively, as the mean and ± 1 standard deviation of 3×3 MODIS AOT retrievals centered at the ARM SGP site. Note, a background AOT of 0.1 is assumed and added to all modeled smoke AOT in the figure (Wang *et al.*, 2006).

We can, however, analyze our system and determine the more and less significant terms and focus on reasonable metrics. We recognize that there is a fairly coarse fundamental observability of the system, particularly at the global scale. In our case, the focal metrics are total particle emissions and AOD (either regionally or by individual grid point). In general, FLAMBE derives reasonable instantaneous correlations of AOD against observations, and even better at the 7 day average. Because in the absence of precipitation, removal for fine mode smoke particles in a region is through transport, we expect and found that AOD linearly scales with emissions. Thus, to first order, we can scale our emissions by the same multiplicative factor. In test simulations, this has been shown to remove the bulk of the bias. Included in the second to last column of Table III are regional multipliers necessary to remove the bulk of the bias by region. The significant digit in these is taken as half integer values. It is our intention to include these multipliers in our next update to the operation emissions model. Because we cannot necessarily determine with certainty what part of the emissions algorithm is incorrect, we are modifying the algorithm to accept these as simple correction factors. Overall, emissions need to be increased by a factor of 1.5–3, with the one exception of sub equatorial Africa, where emissions need to be halved. Tuning such as this can only change the final model performance. The exact value of transfer function from "true" emission to AOD is still unknown. We only know that "input" emissions give us a reasonable output with respect to available observations. True uncertainties are still likely to be quite high. We are particularly concerned with the other side of the smoke budget, namely wet and dry deposition. Based on regional precipitation patterns and the current smoke dry deposition function coupled with preliminary investigations of the DA innovation vectors, we have reason to believe that NAAPS and most other global aerosol models are over scavenging smoke in the tropics, maybe by as much as a factor of two [79].

The last column of Table III presents the annual $\mathrm{PM}_{2.5}$ emissions from GFED [27]. GFED employs a more detailed mechanistic emissions estimation approach, but lacks rigorous emissions validation. The divergent methods of GFED and FLAMBE give insight into the uncertainties in emissions budgets. Half of the regions match within a factor of 2, with FLAMBE usually higher. These include Sahelian Africa, boreal regions, the Indian subcontinent, and insular SE Asia. Differences in Australia, Southern Africa and eastern CONUS are roughly a factor of three.

There are some regions of massive divergence between GFED and FLAMBE, notably East Asia, Peninsular SE Asia, Western CONUS and Europe/Mediterranean. For mid latitude fires, large differences are not unexpected-owing to the difficulty in estimating emissions from individual fires. The results in SE Asia are a result of the combined effects of different treatment of agricultural fires, which are assigned much higher emissions in FLAMBE, and the parameterization of peatland burning in GFED [27], which is not treated explicitly in FLAMBE. Comparison of NAAPS output to surface observations of $\mathrm{PM}_{2.5}$ during an extreme burning event in Indonesia (October 2006) indicates that FLAMBE underestimates smoke in this region [74]. Investigations are ongoing to use newly available peatland datasets to better describe the role of peat burning in regional aerosol in SE Asia.

These differences demonstrate the true observability of the system given available tools and data sets. Global models in general show large differences in outcomes even when emissions are constrained (e.g., AEROCOM-[80]). DA systems are becoming more sophisticated, facilitating direct comparison of bottom-up and top-down inventories. Ultimately, in order to reduce the uncertainties in particle emissions below the integer factor level, these top-down exercises are required, along with transparent bottom-up algorithms permitting realistic, quantitative error propagation.

B. Future Directions

Last, we wish to provide a brief description as to the direction of the FLAMBE project. The next significant challenge is a complete overhaul of the FLAMBE source function. Until recently metadata was not available for WF_ABBA data. In the next generation, we will utilize coverage and cloud masks to generate a probabilistic emissions term. Further, we can also begin to devise methods of fusing multiple products, including dual viewing geostationary and geostationary + polar orbiter.

Within the next two years three additional geostationary satellites with fire monitoring capabilities will become operational providing additional coverage of eastern Europe and Asia. NPOESS VIIRS will serve as follow-on to MODIS. Although fire monitoring has historically not been a primary requirement for operational meteorological satellites, fire detection and characterization is a requirement for NPOESS, GOES-R, and Meteosat Third Generation (MTG). While we believe increases in the number of satellite products will benefit the accuracy of the final simulation, we still have great challenges in the fundamental interpretation of the data. As described in Section III, it took nearly 6 years for the first rigorous analysis of MODIS and GOES product efficacy to be complete. With the tremendous increase in global fire data derived from a diverse set of geostationary and polar orbiting platforms, there is an urgent need for consistent satellite radiometric calibration and fire product characterization activities. It is imperative that programs like FLAMBE join with others to ensure the data and products are properly characterized.

Characterization will no doubt generate a further set of uncertainties leaving us with a fundamental observability of the system. For example, land surface heterogeneity and sensors of finite temporal and spatial resolution are a facts science must cope with. In response, FLAMBE is moving towards probabilistic methods for emissions and ensemble data assimilation. Similarly, FLAMBE will begin to make a series of climatology runs with ever increasing levels of assimilated products including MISR AOD [81] and CALIPSO vertical profiles [67]. Because of its ability to characterize aerosol particles over clouds, the incorporation of the OMI aerosol index into the data assimilation preprocessor is a priority [82], [83]

A new major thrust of FLAMBE is to couple the smoke product to the meteorology. Currently funding is in place to incorporate smoke induced heating rates into meso and global meteorology models. ECMWF has already moved far in his direction.

Last, the better characterization of fire and smoke emission products from FLAMBE will also benefit the research on other environmental aspects of biomass burning. Indeed, $\mathrm{PM}_{2.5}$ accounts for $\sim\ 10\%$ of fires' total emission; CO_2 (greenhouse gases) and CO (primary air pollutant regulated by EPA) contribute the most ($> 80\%$), with the rest of CH_4 and other hydrocarbon gases. Since emissions of these gases are on the first order linearly correlated with $\mathrm{PM}_{2.5}$ emission, an improved FLAMBE emission can be used as a springboard to render a better characterization of the carbon budget. Collaborations are now underway to use FLAMBE emission into global chemistry models to understand the impact of fire emissions on atmospheric chemistry and climate, as well as to refine the source functions of organic aerosol particles. Those improvements in turn enhance the opportunity for inverse modeling of secondary organic production.

VI. Conclusion

In this manuscript, we give an overview of the FLAMBE biomass burning monitoring system and present fundamental metrics on emission and transport patterns of smoke. We also provide short regional assessments of FLAMBE performance. To address fundamental observability issues of the system, FLAMBE needs to be as simple and transparent as possible while still capturing as much of the variance in the system as possible. To this end, FLAMBE uses a fairly straightforward and traceable emissions and transport models. Now coupled with an aerosol optical data assimilation system, FLAMBE can capture the bulk of the variance in large smoke events. Our findings can be summarized as follows.

a) Despite a daunting direct propagation of error in the estimation of emissions from individual fires by satellite, in major burning regions of the globe, the FLAMBE AODs correlate reasonably well with AERONET observations. This is largely due to large spatial autocorrelations of fire activity and compensation of errors among the combined emissions of a large ensemble of fires. But, regional biases in a forward system are to be expected, and appear to be improved with a simple multiplier.

b) Comparison of emissions to GFED is typically within a factor of two or three. That said, there is a great deal of effort required to fully account for all of the parts of the biomass burning system. Some regions however, such as Asia and the mid-latitudes show much larger differences, in some cases as much as an order of magnitude. Regardless, the comparisons demonstrate that emissions algorithms are model dependant. To get a better understanding of "true emissions" requires the propagation of model error-something which is extremely difficult.

c) Smoke AOD and transport simulations can be vastly improved through the use of MODIS optical depth data assimilation– on average halving the variance between model and ground observation in regional or greater scale plumes. This said, proper characterization and error analysis of the satellite data is imperative. Assimilation of over land MODIS AOD clearly increases correlations but some systematic bias persists.

d) Even with data assimilation, the chain between emissions and AOD is not well understood. It appears that emissions linearly correlate with AOD in major burning regions of

the globe. Since the uncertainty in mass extinction efficiency and hygroscopicity of smoke are small relative to emissions, comparison of AOD to emissions is not an unreasonable method to tune emissions estimates. But we can foresee a number of further uncertainties and ultimately we don't believe that at this point we can estimate true emissions within a factor of 2.

e) FLAMBE has the best performance in South America, with instantaneous natural run and data assimilation correlations on the order of 0.75–0.83 and 0.84–0.98, respectively. However, while the natural run model underestimated AOD by 50%, the data assimilation runs overestimates by as much as 50% due to biases in the MODIS AOD product. As AOD scales linearly in emissions, this analysis supports the original suggestion [13] that annual particle emissions in South America likely lie within the 20–30 Tg yr $^{-1}$ range.

f) In Africa, correlations are moderate, on the order of 0.3–0.5 instantaneous and 0.2–0.7 for 7 day averages. Data assimilation makes the most improvement here, increasing correlations to 0.61–0.91 and 0.76–0.95 for instantaneous and 7 day, respectively. Natural FLAMBE runs underestimate AOD and likely emissions in the Sahel by a factor of 2. For Central Africa, FLAMBE overestimates AOD on the order of ~ 2.

g) For Peninsular SE Asia, correlations of AOD to AERONET are good: on the order of 0.47-0.72 (instantaneous) and 0.7-0.73 (7-day). Data assimilation helps with bias removal, but only moderately improves correlations (0.71-0.83 and 0.8-0.87 for instantaneous and 7 day, respectively). This is most likely due to fewer available observations and perhaps cloud bias in the satellite AOD data. There are very few validation sources in insular SE Asia, but based on data assimilation innovations, we believe these correlations are also representative there.

h) Boreal regions show mixed results. FLAMBE can detect and properly model transport of significant boreal fires. However, there is difficulty with emissions magnitudes for individual events. Typically FLAMBE underestimates AOD by a factor of 2-3. But, in general it is difficult to validate boreal smoke, due to few AERONET sites in boreal Asia, and frequent pollution and dust impacts in the surrounding regions. For the two AERONET sites which are dominated by boreal smoke (Bonanza Creek and Bratt's Lake) correlations that range from 0.26-0.49 (instantaneous) to 0.4-0.52 (7-day) are improved by data assimilation to 0.4-53 and 0.76-0.89.

i) For Central America, we do not have any pure smoke AERONET sites for doing a yearly analysis. However, validation with AERONET and surface $\mathrm{PM}_{2.5}$ has been performed on the mesoscale showing good correlation (> 0.7), but with a factor of 2-3 low bias in AODs and surface concentrations. For the global model, this is similar to the assimilation innovations.

j) Isolated mid-latitude fires pose the greatest challenges in that fire properties have less regional covariance and uncertainties can be quite large for isolated events. This is further complicated by a lack of adequate validation data for such events. Surface samplers often do not represent smoke aloft, and remote sensing systems have difficulty retrieving optical depth in thick plumes.

k) Last, the FLAMBE program is continuously expanding, adding more satellite data as they become available. There is a preference for operational data such as those available from geostationary meteorology satellites and later NPOESS. Data is being applied to several ESS problems, notably those related to aerosol-cloud-precipitation interaction.

ACKNOWLEDGMENT

The authors would like to thank NOAA NESDIS for the operational transition and distribution of WF_ABBA. None of the FLAMBE MODIS work would be possible without the effort and community mindedness of the University of Maryland Fire Science Team, including I. Csiszar, L. Giglio, and C. Justice. They would also like to thank the NASA/NOAA Near Real Time Processing Effort for the quasi-operational distribution of NASA products, as well as the investigators of the AERONET program for the use of their data. Last, they would like to thank their many collaborators over the years.

REFERENCES

[1] D. Jaffe, I. Bertschi, L. Jaeglé, P. Novelli, J. S. Reid, H. Tanimoto, R. Vingarzan, and D. L. Westphal, "Long-range transport of Siberian biomass burning emissions and impact on surface ozone in western North America," *Geophys. Res. Lett.*, vol. 31, p. L16106, 2004.

[2] C. M. Rogers and K. P. Bowman, "Transport of smoke from the Central American fires of 1998," *J. Geophys. Res.*, vol. 106, pp. 28,357–28,368, 2001.

[3] J. Wang, S. A. Christopher, U. S. Nair, J. S. Reid, E. M. Prins, J. Szykman, and J. L. Hand, "Mesoscale modeling of Central American smoke transport to the United States: 1. ''Top-down'' assessment of emission strength and diurnal variation impacts," *J. Geophys. Res.*, vol. 111, p. D05S17, 2006.

[4] M. D. Fromm and R. Servranckx, "Transport of forest fire smoke above the tropopause by supercell convection," *Geophys. Res. Lett.*, vol. 30, pp. 1542–1542, 2003.

[5] R. E. Honrath, R. C. Owen, M. Val Martýn, J. S. Reid, K. Lapina, P. Fialho, M. P. Dziobak, J. Kleissl, and D. L. Westphal, "Regional and hemispheric impacts of anthropogenic and biomass burning emissions on summertime CO and O3 in the North Atlantic lower free troposphere," *J. Geophys. Res.*, vol. 109, p. D24310, 2004.

[6] I. Mattis, D. Muller, A. Ansmann, U. Wandinger, J. Preißler, P. Seifert, and M. Tesche, "Ten years of multiwavelength Raman lidar observations of free-tropospheric aerosol layers over central Europe: Geometrical properties and annual cycle," *J. Geophys. Res.*, vol. 113, p. D20202, 2008.

[7] W. McMillan *et al.*, "AIRS views transport from 12 to 22 July 2004 Alaskan/Canadian fires: Correlation of AIRS CO and MODIS AOD with forward trajectories and comparison of AIRS CO retrievals with DC-8 in situ measurements during INTEX-A/ICARTT," *J. Geophys. Res.*, vol. 113, p. D20301, Jul. 2008.

[8] D. L. Westphal and O. B. Toon, "Simulations of microphysical , radiative, and dynamic processes in a continental-scale forest fire smoke plume," *J. Geophys. Res.*, vol. 96, pp. 22,379–22,400, 1991.

[9] E. M. Prins, J. M. Feltz, W. P. Menzel, and D. E. Ward, "An overview of GOES-8 diurnal fire and smoke results for SCAR-B and the 1995 fire season in South America," *J. Geo. Res.*, vol. 103, pp. 31,821–31,836, 1998.

[10] I. Koren, Y. J. Kaufman, L. A. Remer, and J. V. Martins, "Measurement of the effect of Amazon smoke on inhabitation of cloud formation," *Science*, vol. 303, pp. 1342–1345, 2004.

[11] W. A. Lyons, T. E. Nelson, E. R. Williams, J. A. Crarmerand, and T. R. Turner, "Enhanced positive cloud-to-ground lightning in thunderstorms ingesting smoke from fires," *Science*, vol. 282, pp. 77–80, 1998.

[12] J. Wang, S. Van den Heever, and J. S. Reid, "A conceptual model for the linkage between Central American biomass burning aerosols and severe weather over the south central United States," *Environ. Res. Lett.* , p. 015003, 2009, DOI:10.1088/1748-9326/4/1/015003.

[13] J. S. Reid, E. M. Prins, D. L. Westphal, C. C. Schmidt, K. A. Richardson, S. A. Christopher, T. F. Eck, E. A. Reid, C. A. Curtis, and J. P. Hoffman, "Real-time monitoring of South American smoke particle emissions and transport using a coupled remote sensing/box-model approach," *Geophys. Res. Lett.*, vol. 31, p. L06107, 2004.

[14] J. S. Reid, R. Koppmann, T. Eck, and D. Eleuterio, "A review of biomass burning emissions part II: Intensive physical properties of biomass burning particles," *Atmos. Chem. Phys.*, vol. 5, pp. 799–825, 2005.

[15] E. M. Prins and W. P. Menzel, "Trends in South-American biomass burning detected with the goes visible infrared spin scan radiometer atmospheric sounder from 1983 to 1991," *J. Geophys. Res.-Atmos.*, vol. 99, pp. 16719–16735, 1994.

[16] E. Prins, J. Schmetz, L. Flynn, D. Hillger, and J. Feltz, "Overview of current and future diurnal active fire monitoring using a suite of international geostationary satellites," in *Global and Regional Wildfire Monitoring: Current Status and Future Plans*, F. J. Ahern, J. G. Goldammer, and C. O. Justice, Eds. The Hague, Netherlands: SPB Academic Publishing, 2001, pp. 145–170.

[17] E. M. Prins, C. C. Schmidt, J. M. Feltz, J. S. Reid, D. L. Wesphal, and K. Richardson, "A two-year analysis of fire activity in the Western Hemisphere as observed with the GOES wildfire automated biomass burning algorithm," in *Proc. 12th Conf. Satellite Meteorology and Oceanography*, Long Beach, CA, 2001, Amer. Meteor. Soc., p. P2.28, (preprints).

[18] C. S. Schmidt and E. Prins, "GOES wildfire applications in the Western Hemisphere," in *Proc. 2nd Int. Wildland Fire Ecology and Fire Management Congr. AMS 5th Symp. Fire and Forest Meteorology*, Orlando, FL, Nov. 16–20, 2003, p. 4.

[19] L. Giglio, J. Descloitres, C. O. Justice, and Y. J. Kaufman, "An enhanced fire detection algorithm for MODIS," *Remote Sens. Environ.*, vol. 87, pp. 273–282, 2003.

[20] L. Giglio, I. Csiszar, and C. O. Justice, "Global distribution and seasonality of active fires as observed with the Terra and Aqua Moderate Resolution Imaging Sepctroradiometer (MODIS) sensors," *J. Geophys. Res.*, vol. 111, p. G02016, 2006.

[21] J. A. Dozier, "Methods for satellite identification of surface temperature fields of subpixel resolution," *Remote Sens. Environ.*, vol. 11, pp. 221–229, 1981.

[22] C. L. Heald, D. J. Jacobs, P. I. palmer, M. J. Evans, G. W. Sachse, H. B. Singh, and D. R. Blake, "Biomass burning emissions inventory with daily resolution: Application to aircraft observations and Asian outflow," *J. Geophys. Res.*, vol. 108, p. 8811, 2003.

[23] W. Schroeder, J. T. Morisette, I. Csiszar, L. Gigliom, D. Morton, and C. O. Justice, "Characterizing vegetation fire dynamics in Brazil through multisatellite data: Common trends and practical issues," *Earth Interactions*, vol. 9.13, pp. 1–26, 2005.

[24] M. J. Wooster, B. Zhukov, and D. Oertel, "Fire radiative energy for quantitative study of biomass burning: Derivation from the BIRD experimental satellite and comparison to MODIS fire products," *Remote Sens. Environ.*, vol. 86, pp. 83–107, 2003.

[25] C. Ichoku and Y. J. Kaufman, "A method to derive smoke emission rates from MODIS fire radiative energy measurements," *IEEE Trans. Geosci. Remote Sens.*, vol. 43, pp. 2636–2649, 2005.

[26] L. Giglio and J. D. Kendall, "Application of the Dozier retrieval to wildfire characterization-A sensitivity analysis," *Remote Sens. Environ.*, vol. , 77, pp. 34–49, 2001.

[27] G. R. Van der Werf, J. T. Randerson, L. Giglio, G. L. Collatz, P. S. Kasibhatta, and A. F. Arellano, "Interrannual variability in global biomass burning emissions from 1997 to 2004," *Atmos. Chem. Phys.*, vol. 6, pp. 3423–3441, 2006.

[28] T. F. Eck *et al.*, "Optical properties of boreal region biomass burning aerosols in central Alaska and seasonal variation of aerosol optical depth at an Arctic coastal site," *J. Geophys. Res.*, 2009, DOI:10.1029/2008JD010870, to be published.

[29] T. J. Hawbaker, V. C. Radeloff, A. D. Syphard, Z. L. Zhu, and S. I. Stewart, "Detection rates of the MODIS active fire product in the United States," *Remote Sens. Environ.*, vol. 112, pp. 2656–2664, 2008.

[30] M. Theisen, E. Prins, C. Schmidt, J. S. Reid, J. Hunter, and D. Westphal, "Data filtering of Western Hemisphere GOES wildfire ABBA products," in *Eos Trans. AGU*, 2002, vol. 83(19), Spring Meet. Suppl., Abstract A21B-10.

[31] L. Giglio, "Characterization of the tropical diurnal fire cycle using VIRS and MODIS observations," *Remote Sens. Environ.*, vol. 108, pp. 407–421, 2007.

[32] X. Zhang and S. Kondragunta, "Temporal and spatial variability in biomass burned area aross the USA derived from the GOES fire product," *Remote. Sens. Environ.*, vol. 112, pp. 2886–2897, 2008.

[33] W. Schroeder, E. Prins, L. Giglio, I. Csiszar, C. Schmidt, J. Morissette, and D. Morton, "Validation of GOES and MODIS active fire detection products using ASTER and ETM plus data," *Remote Sens. Environ.*, vol. 112, pp. 2711–2726, 2008.

[34] W. Schroeder, *Towards an Integrated System for Vegetation Fire Monitoring in the Amazon Basin, Dissertation*. : Dept. Geography, Univ. Maryland, 2008, vol. #5348, pp. 1–182.

[35] P. J. Crutzen and M. O. Andreae, "Biomass burning in the tropics: Impacts on atmospheric chemistry and biogeochemical cycles," *Science*, vol. 250, pp. 1669–1678, 1990.

[36] T. R. Loveland, B. C. Reed, J. F. Brown, D. O. Ohlen, Z. Zhu, L. Yang, and J. W. Merchant, "Development of a global land cover characteristics database and IGBP DISCover from 1 km AVHRR data," *Int. J. Remote Sens.*, vol. 21, pp. 1303–1330, 2000.

[37] L. S. Guild, J. B. Kauffman, L. J. Ellingson, D. L. Cummings, E. A. Castro, R. E. Babbitt, and D. E. Ward, "Dynamics associated with total aboveground biomass, C, nutrient pools, and biomass burning of primary forest and pasture in Rondonia, Brazil during SCAR-B," *J. Geophys. Res.*, vol. 24, pp. 32,091–32,100, 1998.

[38] E. J. Hyer and J. S. Reid, "Baseline uncertainties in biomass burning emission models resulting from spatial error in satellite active fire location data," *Geophys. Res. Lett.*, vol. 36, p. L05802, 2009.

[39] W. Schroeder, I. Csiszar, and J. Morisette, "Quantifying the impact of cloud obscuration on remote sensing of active fires in the Brazilian Amazon," *Remote Sens. Environ.*, vol. 112, pp. 456–470, 2008.

[40] J. H. Christensen, "The Danish eulerian hemispheric model-A three dimensional air pollution model used for the arctic," *Atmos. Environ.*, vol. 24, pp. 4169–4191, 1997.

[41] T. F. Hogan and T. E. Rosmond, "The description of the Navy Operational Global Atmospheric Prediction Systems spectral forecast model," *Month. Weather Rev.*, vol. 119, pp. 1786–1815.

[42] T. F. Hogan and L. R. Brody, "Sensitivity studies of the Navy global forecast model: Parameterizations and evaluation of improvements in NOGAPS," *Month. Weather Rev.*, vol. 121, pp. 2372–2395, 1992.

[43] I. Uno *et al.*, "Dust model intercomparison (DMIP) study over Asia: Overview," *J. Geophys. Res.*, vol. 111, p. D12213, 2006.

[44] M. Witek, P. J. Flatau, P. K. Quinn, and D. L. Westphal, "Global sea-salt modeling: Results and validation against multicampaign shipboard measurements," *J. Geophys. Res.*, vol. 112, p. D08215, 2007.

[45] A. Staniforth and J. Cote, "Semi-Lagrangian integration schemes for atmospheric models—A Review," *Month. Weather Rev.*, vol. 119, pp. 2206–2223, 1991.

[46] H. Ritchie, "Semi-lagrangian advection on a Gaussian grid," *Month. Weather Rev.*, vol. 115, pp. 608–619, 1987.

[47] J. S. Reid, P. V. Hobbs, R. J. Ferek, J. V. Martins, D. R. Blake, M. R. Dunlap, and C. Liousse, "Physical, chemical, and radiative characteristics of the smoke dominated regional hazes over Brazil," *J. Geophys. Res.*, vol. 103, pp. 32,059–32,080, 1998.

[48] B. I. Magi, P. V. Hobbs, B. Schmid, and J. Redemann, "Vertical profiles of light scattering, light absorption, and single scattering albedo during the dry, biomass burning season in southern Africa and comparisons of in situ and remote sensing measurements of aerosol optical depths," *J. Geophys. Res.*, vol. 108(D13), p. 8504, 2003.

[49] R. A. Kahn, Y. Chen, D. L. Nelson, F.-Y. Leung, Q. Li, D. J. Diner, and J. A. Logan, "Wildfire smoke injection heights: Two perspectives from space," *Geophys. Res. Lett.*, vol. 35, p. L04809, 2008.

[50] B. Yan, M. Zheng, Y. T. Hu, S. Lee, H. K. Kim, and A. G. Russell, "Organic composition of carbonaceous aerosols in an aged prescribed fire plume," *Atmos. Chem. Phys.*, vol. 8, pp. 6381–6394, 2008.

[51] J. S. Reid, T. Eck, S. Christopher, O. Dubovik, R. Koppmann, D. Eleuterio, B. Holben, E. Reid, and J. Zhang, "A review of biomass burning emissions part III: Intensive optical properties of biomass burning particles," *Atmos. Chem. Phys.*, vol. 5, pp. 827–849, 2005.

[52] R. A. Kotchenruther and P. V. Hobbs, "Humidification factors of aerosols from biomass burning in Brazil," *J. Geophys. Res.*, vol. 103, pp. 32,081–32,089, 1998.

[53] J. Cook, M. Frost, G. Love, L. Phegley, Q. Zhao, D. Geiszler, J. Kent, S. Potts, D. Martinez, T. Neu, D. Dismachek, and L. McDermid, "The U.S. Navy's on-demand, coupled, mesoscale data assimilation and prediction system," in *Proc. 22nd Conf. Weather Analysis and Forecasting/ 18th Conference on Numerical Weather Prediction*, Park City, UT, Jun. 25–29, 2007.

[54] R. M. Hodur, "The Naval Research Laboratory's coupled ocean atmosphere mesoscale prediction system (COAMPS)," *Month. Weather Rev.*, vol. 125, pp. 1414–1430, 1997.

[55] J. Wang, "Air Quality and Radiative Impacts of Long-Range Transported Aerosols Over the Southeastern United States," Ph.D. dissertation, Dept. Atmos. Sci., Univ. Alabama, Huntsville, 2005.

[56] R. A. Pielke, R. L. Walko, J. L. Eastman, W. A. Lyons, R. A. Stocker, M. Uliasz, and C. J. Tremback, "A comprehensive meteorological modeling system—RAMS," *Meteor. Atmos. Phys.*, vol. 49, pp. 69–91, 1992.

[57] W. R. Cotton, R. A. Pielke, R. L. Walko, G. E. Liston, C. J. Tremback, H. Jiang, R. L. McAnelly, J. Y. Harrington, M. E. Nicholls, G. G. Carrio, and J. P. McFadden, "RAMS 2001: Current status and future directions," *Meteor. Atmos. Phys.*, vol. 82, pp. 5–29, 2003.

[58] Q. Fu and K. N. Liou, "Parameterization of the radiative properties of cirrus clouds," *J. Atmos. Sci.*, vol. 50, pp. 2008–2025, 1993.

[59] J. Wang, U. Nair, and S. A. Christopher, "GOES-8 aerosol optical thickness assimilation in a mesoscale model: Online integration of aerosol radiative effects," *J. Geophys. Res.*, vol. 109, 2004, DOI:10.1029/2004JD004827.

[60] J. Wang and S. A. S. A. Christopher, "Mesoscale modeling of Central American smoke transport to the United States: 2. Smoke radiative impact on regional surface energy budget and boundary layer evolution," *J. Geophys. Res.*, vol. 111, p. D14S92, 2006.

[61] F. Patadia, P. Gupta, S. A. Christopher, and J. S. Reid, "A multi-sensor satellite based assessment of biomass burning aerosol radiative impact over Amazonia," *J. Geophys. Res.*, vol. 113, p. D12214, 2008.

[62] J. Zhang, J. S. Reid, D. L. Westphal, N. Baker, and E. J. Hyer, "A system for operational aerosol optical depth data assimilation over global oceans," *J. Geophys. Res.*, vol. 113, p. D10208, 2008.

[63] L. A. Remer, Y. J. Kaufman, D. Tanré, S. Mattoo, D. A. Chu, J. V. Martins, Li R.-R, C. Ichoku, R. C. Levy, R. G. Kleidman, T. F. Eck, E. Vermote, and B. N. Holben, "The MODIS aerosol algorithm, products and validation," *J. Atmos. Sci.*, vol. 62, pp. 947–973, 2005.

[64] J. Zhang and J. S. Reid, "MODIS aerosol product analysis for data assimilation: Assessment of over-ocean level 2 aerosol optical thickness retrievals," *J. Geophys. Res.*, vol. 111, p. D22207, 2008.

[65] R. C. Levy, L. A. Remer, S. Mattoo, E. F. Vermote, and Y. J. Kaufman, "Second-generation operational algorithm: Retrieval of aerosol properties over land from inversion of Moderate Resolution Imaging Spectroradiometer spectral reflectance," *J. Geophys. Res.*, vol. 112, p. D13211, 2007.

[66] B. N. Holben *et al.*, "AERONET- A federated instrument network and data archive for aerosol characterization," *Remote Sens. Environ.*, vol. 66, pp. 1–6, 1998.

[67] J. R. Campbell, J. S. Reid, D. L. Westphal, J. Zhang, E. J. Hyer, and E. J. Welton, "CALIOP aerosol subset processing for global aerosol transport model data assimilation," *J. Sel. Topics Appl. Earth Obs. Rem. Sens.*, 2009, submitted for publication.

[68] N. T. O'Neill, T. F. Eck, A. Smirnov, B. N. Holben, and S. Thulasiraman, "Spectral discrimination of coarse and fine mode optical depth," *J. Geophys. Res.*, vol. 108, p. 4559, 2003.

[69] B. E. Anderson *et al.*, "Aerosols from biomass burning over the tropical south Atlantic region: Distributions and impacts, 1996," *J. Geophys. Res.*, vol. 101, pp. 24,117–24,137, 1996.

[70] R. J. Swap, H. J. Annegarn, J. T. Suttles, M. D. King, S. Platnick, J. L. Privette, and R. J. Scholes, "Africa burning: A thematic analysis of the Southern African Regional Science Initiative (SAFARI 2000)," *J. Geophys. Res.*, vol. 108(D13), p. 8465, 2003.

[71] J. Zhang and J. S. Reid, "An analysis of clear sky and contextual biases using an operational over ocean MODIS aerosol product," *Geophys. Res. Lett.*, 2009, submitted for publication.

[72] N. T. O'Neill, N. T. M. Campanelli, A. Lumpu, S. Thulasiraman, J. S. Reid, M. Aube, L. Nearly, J. W. Kaminski, and J. C. McConnell, "Optical evaluation of the GEM-AQ air quality model during the Quebec smoke event of 2002; performance criteria for extensive and intensive optical variables," *Atmos. Environ.*, vol. 40, pp. 3737–3749, 2006.

[73] N. T. O'Neill, O. Pancrati, K. Baibakov, E. Eloranta, R. L. Batchelor, J. Freemantle, L. J. B. McArthur, K. Strong, and R. Lindenmaier, "Occurrence of weak, sub-micron, tropospheric aerosol events at high Arctic latitudes Occurrence of weak, sub-micron, tropospheric aerosol events at high Arctic latitudes," *Geophys. Res. Lett.*, vol. 35, p. L14814, 2008.

[74] E. J. Hyer and B. N. Chew, "Aerosol transport model evaluation of an extreme smoke episode in Southeast Asia," *Atmos. Environ.*, 2009, submitted for publication.

[75] D. H. Levinson and A. M. Waple, "State of the climate 2003," *Bull. Amer. Meteor. Soc.*, vol. 85, pp. S1–S72, 2004.

[76] J. L. McCarty, C. O. Justice, and S. Korontzi, "Agricultural burning n the Southeastern United States detected by MODIS," *Remote Sens. Environ.*, vol. 108, 2007.

[77] D. McNamara, G. Stephens, and M. Ruminski, "The Hazard Mapping System (HMS) – NOAA multi-sensor fire and smoke detection program using environmental satellites," in *13th Conf. Satellite Meteorology and Oceanography*, Norfolk, VA, 2004, Amer. Meteor. Soc., 4.3, (preprints).

[78] X. Zhang, S. Kondragunta, C. Schmidt, and F. Kogan, "Near real time monitoring of biomass burning particulate emissions (PM2.5) across contiguous United States using multiple satellite instruments," *Atmos. Environ.*, vol. 42, pp. 6959–6971, 2008.

[79] P. Xian, J. S. Reid, J. F. turk, E. J. Hyer, and D. L. Westphal, "Impact of modeled versus satellite measured tropical precipitation on regional smoke optical thickness in an aerosol transport model," *Geophys. Res. Lett.*, 2009, submitted for publication.

[80] C. Textor *et al.*, "Analysis and quantification of the diversities of aerosol life cycles within AeroCom," *Atmos. Chem. Phys.*, vol. 6, pp. 1777–1813, 2006.

[81] Y. Shi, J. Zhang, and J. S. Reid, "Development of the data assimilation quality MODIS and MISR aerosol products for data integration and assimilation," *Eos Trans.*, vol. 89, Fall meet. Suppl., Abstract A21G-04.

[82] C. Anh, O. Torres, and P. K. Bartia, "Comparison of ozone monitoring UV aerosol products with Aqua/Moderate Resolution Imaging Spectroradiometer and Multiangle Imaging Spectroradiometer observations in 2006," *J. Geophys. Res.*, vol. 113, p. D16S27, 2006.

[83] J. S. Reid, J. Zhang, C. Hsu, S. A. Christopher, E. J. Hyer, A. P. Kuciaskas, D. L. Westphal, and J. A. Hansen, "Application of multi-sensor fusion to the aerosol forecasting problem," in *Eos Trans. AGU*, 2007, vol. 88, Fall Meet. Suppl., Abstract A11E-03.

[84] W. P. Menzel and J. F. W. Purdom, "Introducing GOES-I: The first of a new generation of geostationary operational environmental satellites," *Bull. Amer. Meteor. Soc.*, vol. 75, pp. 757–781, 1994.

[85] J. Schmetz, P. Pili, S. Tjemkes, D. Just, J. Kerkman, S. Rota, and A. Ratier, "An introduction to Meteosat second generation (MSG)," *Bull. Amer. Meteor. Soc.*, vol. 83, pp. 977–992, 2002.

[86] E. M. Prins, I. Csiszar, W. Shroeder, C. Schmidt, L. Giglio, J. Hoffman, M. Wooster, J. Reid, E. Hyer, and Y. Govaerts, Global Geostationary Fire Monitoring: Sensor and Data Issues and Recommendations 2008, CGMS-36, NOAA-WP-21.

Jeffrey S. Reid received the B.S. degree in applied physics, the M.S. degree in atmospheric science from the University of California, Davis, and the Ph.D. degree from the Atmospheric Sciences Department, University of Washington, in 1993, with a dissertation topic on the emission, evolution and radiative impacts of biomass burning smoke.

He performed research at the Crocker Nuclear Lab on the nuclear analysis of aerosol particles, atmospheric radiation, air quality, and inhalation toxicology/epidemiology. Upon completion, he accepted a position at the U.S. Navy's Space and Naval Warfare Systems Center, San Diego, CA, where he began a program on operational model/satellite product validation for aerosol forecasting and initiated the FLAMBE program. In 2002, he joined the Naval Research Laboratory Marine Meteorology Division, Monterey, CA, where he now leads a research group on aerosol observability in the Aerosol and Radiation Section.

Edward J. Hyer received the B.A. degree in chemistry from Goucher College and the M.A. and Ph.D. degrees in geography from the University of Maryland, College Park.

Currently, he is a UCAR Project Scientist working at the naval Research laboratory Marine Meteorology Division on observations and modeling of biomass burning emissions. He is currently the lead emissions developer of the FLAMBE system.

Elaine M. Prins received the B.S. degree in atmospheric science from the University of California, Davis, in 1985, and the M.S. degree in meteorology from the University of Wisconsin (UW), Madison, in 1989.

For the past 17 years, she has collaborated with the UW-Madison Cooperative Institute for Meteorological Satellite Studies (CIMSS) as a CIMSS employee, and as a member of the NOAA NESDIS Advanced Satellite Products Branch (ASPB) from 1996 to 2004. As a NESDIS research scientist, she was responsible for geostationary satellite investigations of biomass burning and served as the principle investigator of the GOES biomass burning remote sensing program. She currently serves as a consultant for CIMSS. She participates in international environmental satellite instrument design and applications studies and is coordinating the GOFC/GOLD global geostationary fire monitoring system development effort. She is also involved in next generation GOES-R fire monitoring design and development activities.

Douglas L. Westphal, photograph and biography not available at the time of publication.

Jianglong Zhang, photograph and biography not available at the time of publication.

Jun Wang received the B.S. degree in metrology from the Nanjing Institute of Meteorology, the M.S. degree in atmospheric dynamics from the Institute of Atmospheric Physics, Chinese Academy of Sciences, and the Ph.D. degree in atmospheric science from the University of Alabama, Huntsville, in 2005, under the support of NASA Earth System Sciences graduate fellowship.

He was a postdoctoral researcher at Harvard University, Cambridge, MA, in 2005–2007, under the support of NOAA Climate and Global Change postdoctoral fellowship. He has been an Assistant Professor at the University of Nebraska, Lincoln, since August 2007. His past research included algorithm development for retrieving optical depth of nonspherical dust particles from geostationary satellites and model development for assimilating satellite-based aerosol products into mesoscale meteorology models to study aerosol radiative impact on weather. His current research focuses on the integration of satellite remote sensing and chemistry transport model to study air quality and aerosol-cloud interaction.

Dr. Wang received the NASA Earth Science New Investigator Award while he was a visiting scientist at the NASA Goddard Space Flight Center in 2008.

Sundar A. Christopher received the M.S. degree in meteorology from South Dakota School of Mines and Technology, the M.S. degree in Industrial/Organizational Psychology from the University of Alabama, Huntsville (UAH), and the Ph.D. degree in atmospheric sciences from Colorado State University.

He is currently a Professor in the Department of Atmospheric Sciences. UAH, and the Associate Director of the Earth System Science Center, UAH. His research interests include satellite remote sensing of clouds and aerosols and their impact on air quality, global, and regional climate.

Cynthia A. Curtis, photograph and biography not available at the time of publication.

Christopher C. Schmidt, photograph and biography not available at the time of publication.

Daniel P. Eleuterio is a Meteorologist and Program Officer at the Office of Naval Research, Arlington, VA. His primary research interests are tropical and mesoscale meteorology and oceanography, marine aerosols, numerical weather prediction, and air-sea interaction.

Kim A. Richardson, photograph and biography not available at the time of publication.

Jay P. Hoffman, photograph and biography not available at the time of publication.